

From single trees to country-wide maps: Modeling mortality rates in Germany based on the Crown Condition Survey

Nikolai Knapp^{a,*}, Nicole Wellbrock^a, Judith Bielefeldt^a, Petra Dühnelt^a, Rainer Hentschel^b, Andreas Bolte^{a,c}

^a Thünen Institute of Forest Ecosystems, Alfred-Möller-Str. 1, Eberswalde 16225, Germany

^b Landeskoppenzentrum Forst Eberswalde (LFE), Alfred-Möller-Str. 1, Eberswalde 16225, Germany

^c Department of Silviculture and Forest Ecology of the Temperate Zones, University of Göttingen, Büsgenweg 1, Göttingen 37077, Germany



ARTICLE INFO

Keywords:

Tree mortality
Drought
Logistic regression
Mapping
Crown condition survey
Forest monitoring

ABSTRACT

Most years in the period from 2018 to 2022 have been exceptionally dry in Central Europe. In Germany's forests, this long-lasting drought has caused unprecedented tree mortality. Systematic ground-based surveys, such as the annual Crown Condition Survey, provide information on the vitality status of the different tree species and their mortality rates. However, models are needed to be able to map the spatial patterns of mortality for each tree species based on cause-effect relationships derived from field observations. In this study, logistic regression models were used to identify the most important drivers of mortality for the most important tree species in Germany. For this purpose, the dead and surviving trees from the Crown Condition Survey were combined with a large set of potential predictor variables from the domains of climate, topography, soil, land cover and deposition. After feature selection, the models were evaluated using the area under the curve (AUC) statistic. Norway spruce (*Picea abies*; AUC = 0.9) showed by far the greatest increase in mortality, with the country-wide average observed and predicted rates approaching almost 10% per year from 2020 to 2022, and much higher predicted rates at the regional level. Much of the spruce mortality was explained by the climatic water balance of the driest summer in previous years. The other main tree species also showed clear mortality responses to the drought conditions. However, in the case of European beech (*Fagus sylvatica*; AUC = 0.94) and Pedunculate and Sessile oak (*Quercus robur* and *petraea*; AUC = 0.88), the peaks in the time series of the country-wide mortality rates stayed below 1%. For these broadleaved species, mortality was more dependent on a range of site conditions, i.e., soil and topography. For Scots pine (*Pinus sylvestris*; AUC = 0.76), for which the observed mortality rate peaked at 1.2% in 2020, the given drivers could explain mortality only to a lesser degree than for the other species. The regression models were used for spatial prediction to produce country-wide maps of species-specific mortality rates at annual temporal and 100-m spatial resolution, covering all years from 1998 to 2022. The maps visualize the spatial patterns of mortality over time. The regions in western and central Germany, which were most seriously affected by spruce dieback can clearly be identified. The models and maps presented can be used for risk assessment, forest planning, and tree species selection, providing decision support for forest practitioners.

1. Introduction

Forest landscapes in Germany have been undergoing dramatic changes for several years since 2017. The cyclones Xavier (October 2017) and Friederike/David (January 2018) caused enormous wind damage and were followed by severe multi-year heat and drought conditions from 2018 to 2020 and again in 2022, accompanied by high insect and pathogen pressure. Historical extreme events, like cyclones in

1973, 1976, 1990, 2000 and 2007, or the summer heat wave of 2003, have left their marks in Germany's forests, but were of short duration with mortality rates quickly returning back to normal (Spathelf et al., 2022). The spatial and temporal extent of the decisive multi-year drought was unprecedented in the European weather records (Rakovcic et al., 2022). The drought has caused massive losses of canopy cover in several central European countries (Senf and Seidl, 2021a).

In Germany, from 2018 to the end of 2022, the unplanned mortality-

* Corresponding author.

E-mail address: nikolai.knapp@thuenen.de (N. Knapp).

related wood volume amounted to around 255 million m³ (233 million m³ of conifers and 22 million m³ of broadleaves) (BMEL, 2023a). This is massive considering that the long term average annual wood harvest in the country amounts to 73 million m³ (BMEL, 2021). The average annual unplanned damage-induced harvest rose from previously 8 million m³ (2010–2017) to 47 million m³ (2018–2022) (Statistisches Bundesamt Destatis, 2023). Approximately 500,000 ha of forest area will need reforestation with a strong focus on previously uniform stands dominated by Norway spruce (*Picea abies*) (BMEL, 2023a). Although exceptional compared to historical conditions, such severe heat waves and droughts are becoming increasingly more likely with climate change (Knutzen et al., 2023). Continued increases in temperature and atmospheric vapor pressure deficit are expected to lead to water and heat stress, with the effects of early leaf shedding, crown dieback and increased mortality rates, altering forest structure and tree species communities in the long term (McDowell et al., 2020). Cases of such elevated mortality rates have been reported from different forest ecosystems around the world (Hartmann et al., 2022). A multi-species synthesis showed that drought-induced tree mortality is associated with hydraulic failure of the xylem tissue (Adams et al., 2017).

In addition to causing physiological stress due to heat and drought, climate change is also altering forest disturbance regimes (Seidl et al., 2017) and the competitive vigor of tree species, leading to shifts in species' suitable distribution ranges (Bolte et al., 2009; Stojnić et al., 2018). Over the past decades, European forests have experienced increasing trends in canopy mortality (Senf et al., 2018) and wood volume lost due to disturbances (Patacca et al., 2023). This applies to the directly weather-related disturbance agents such as wind and fire, which show a stochastic but intensifying pattern of occurrence. It also applies to other abiotic and biotic drivers and stressors such as drought, insects and pathogens, which show steady increases (Anderegg et al., 2015; Patacca et al., 2023). In particular, bark beetles benefit from faster ontogenetic development under warmer temperatures and weakened host trees, leading to many outbreaks in recent years (Hlásny et al., 2021).

The vitality of forests is a topic of great concern to German society.

Almost a third of the country is covered by forests. They provide numerous ecosystem services and are an important economic factor. The forestry and wood products sector is responsible for 735,000 jobs and an annual sales volume of 135 billion € (BMEL, 2021). When dieback caused by sulfur deposition from industrial emissions shattered Germany's forests in the 1980s, the Crown Condition Survey (Waldbestandserhebung, WZE) was initiated as part of the ICP Forests program to monitor tree vitality on an annual basis (Schwarzel et al., 2022; Wellbrock et al., 2018). Following the successful implementation of countermeasures, from the Convention on Long-range Transboundary Air Pollution to soil protection liming, forests were able to recover in the past decades (de Vries et al., 2014; Wellbrock et al., 2016). However, after the drought year 2018, the WZE recorded a rapid and strong deterioration of forest condition, with no recovery up until this study (BMEL, 2023b). Following the ICP Forests standard, tree vitality in the WZE is quantified in terms of crown defoliation. Every survey tree is assessed visually by a team of experts using binoculars and a reference photo booklet. The experts assign each tree to a defoliation class, which describes the percentage of foliage missing (or brown and dead) with regard to a vital reference tree. Each class has a width of 5%. A fully vital tree has 0% defoliation, a tree with a defoliation above 25% is considered severely damaged and a value of 100% marks a dead tree. Several indicators of forest condition entered a plateau phase around new all-time highs in 2019–2022. Average crown defoliation increased from 20% to 26%, the proportion of severely damaged trees (with defoliation > 25%) increased from around 25 to 35%, the average mortality rate (standing dead trees only) increased from 0.2% to 1.4% and the total annual loss rate, including windthrow, salvage logging and planned harvest, which had long been below 3%, increased to over 5% (Fig. 1) (Thünen Institute, 2023). In particular, Norway spruce, which has been planted in many parts of Germany at altitudes below its natural range, is suffering from hot and dry conditions (Bolte et al., 2021).

Given these developments and the need to adapt forests to future climate change, it is necessary to understand which trees of which species are dying, where, and why. Different approaches to studying tree mortality serve different purposes and complement each other. In situ

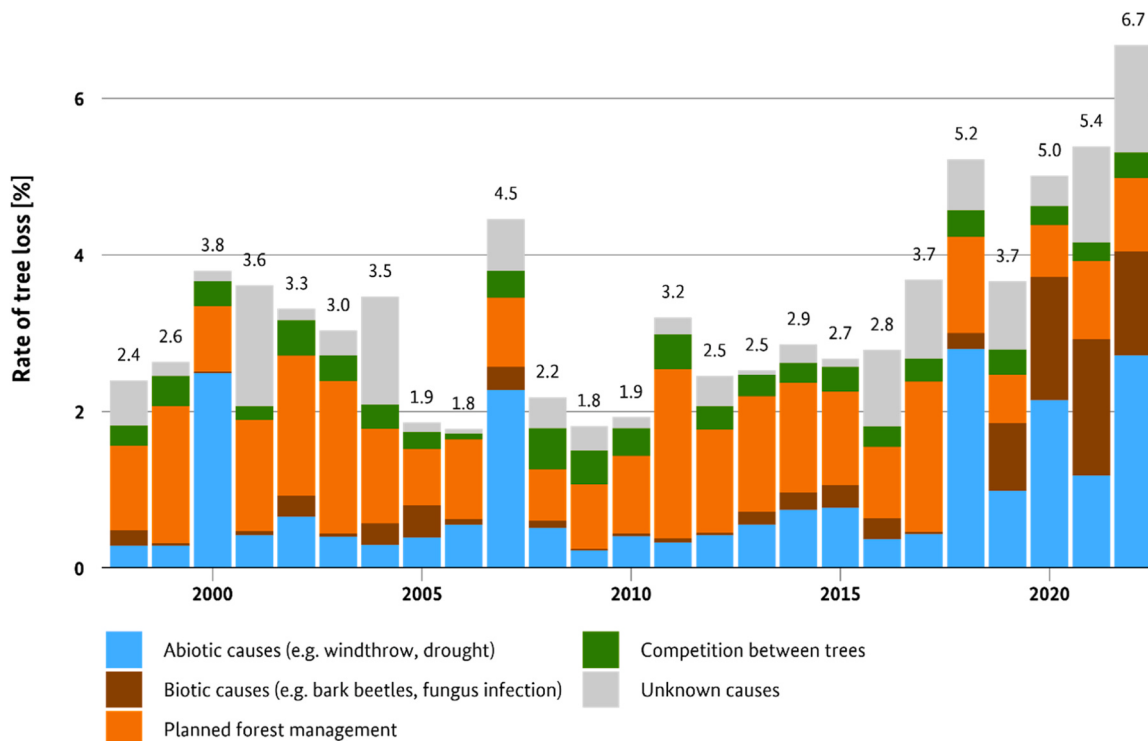


Fig. 1. Annual rates of tree loss from the German Crown Condition Survey, colored according to different causes of loss (BMEL, 2023b; Thünen Institute, 2023).

experiments allow the physiological processes leading to tree deaths to be studied under controlled conditions (Hammond et al., 2019; Sevanto et al., 2014). Remote sensing allows wall-to-wall mapping of areas with canopy cover loss (Senf and Seidl, 2021a; Thonfeld et al., 2022). Large-scale monitoring networks of field plots allow to capture spatial and temporal trends at the species level across the entire environmental feature space where a species occurs (George et al., 2022; Michel et al., 2022). Statistical modeling allows the relationships between environmental drivers and observed mortality to be captured and used for spatiotemporal prediction of mortality risk (Neumair et al., 2022; Taccaen et al., 2022). Ultimately, process-based modeling can integrate knowledge gained at different levels, allowing for mechanistic predictions of mortality under novel environmental conditions (Brodrribb et al., 2019; Bugmann et al., 2019).

In this study, the long-term monitoring data of the Crown Condition Survey were combined with a wide range of environmental variables, all of which could potentially be drivers of tree mortality. The objectives of the study were 1) to assess which tree species are affected by elevated tree mortality, 2) to investigate how accurately mortality of different tree species can be modeled using logistic regression, 3) to map tree mortality in Germany for all years from 1998–2022 at 100-m resolution, and 4) to identify the main environmental drivers of mortality for each species.

2. Material and methods

2.1. Tree mortality data

Field data from the German National Crown Condition Survey (Waldzustandserhebung, WZE) from the years 1998–2022 were used. The WZE monitors approximately 10,000 trees at about 410 plot locations on a regular 16 km × 16 km grid across Germany every year during the summer months between July and September (Wellbrock et al., 2018). The main observable is crown defoliation, which is assessed for the same sample trees every year (Eichhorn et al., 2020). Since 1998, the causes for loss have been recorded for trees that have left the sample. The recordings contain information about whether a dead tree was found standing, lying or removed and whether the loss can be attributed to a planned forest management operation, competition from neighboring trees or a biotic or an abiotic damage agent. Based on this information, each tree in each year was labeled as either surviving or dying. Mortality rates in managed forests can vary widely depending on whether forest management activities are considered mortality events or not (Lech and Kamińska, 2024). In this study, harvested trees and windthrow were excluded. A tree was labeled as dying, if it had still been alive in the previous year and was either standing dead with fine twigs still present but 100% defoliated (tree status 0 or 9 according to Wellbrock et al., 2018) or leaving the WZE sample collective as a dead tree with a natural cause of death, including sanitary logging after biotic infestation (tree status 12, 32, 33, 34, 42 or plot status 12).

2.2. Environmental predictors

The following sections describe the data sources and processing steps for the environmental variables from the different domains climate, topography, soil, land cover and deposition. There are other variables such as forest structure and individual tree attributes that are known to influence tree vitality. An explanation of why these variables were either not available in the required detail or were not appropriate for the specific purpose of this study can be found in Section 4.4. In order to harmonize all environmental data sets, Germany was divided into 3872 tiles of 10 km × 10 km size according to the INSPIRE 10-km grid (BKG, 2018) and using the ETRS89 Lambert Azimuthal Equal-Area projection coordinate reference system (LAEA, EPSG:3035). For each tile and each environmental predictor domain, a data cube (NetCDF file) was created with the spatial dimensions ‘easting’ and ‘northing’ at 100-m cell

resolution (1000-m for climate data) and a ‘time’ dimension for dynamic variables. Processing was mostly done in R (R Core Team, 2021) primarily using the packages data.table (Dowle and Srinivasan, 2023), terra (Hijmans, 2022), sf (Pebesma, 2018) and ncdf4 (Pierce, 2019).

2.2.1. Climate

Climate metrics were computed based on the monthly gridded data from the German Weather Service with a resolution of 1000 m (source: Deutscher Wetterdienst, DWD Climate Data Center, 2023). The following seasonal aggregates were calculated for winter (Dec-Feb), spring (Mar-May), summer (Jun-Aug) and autumn (Sep-Nov) of each year since 1991: 3-month mean of mean temperature, 3-month maximum of maximum temperature, 3-month minimum of minimum temperature, 3-month sums of precipitation, potential and actual evapotranspiration (PET and AET) (Allen et al., 1998). The climatic water balance (CWB) was calculated as the difference between precipitation and potential evapotranspiration. Precipitation and evapotranspiration are due to different meteorological cause often not the same either in amount or distribution (Thornthwaite, 1948) and CWB is proposed to represent the climatic conditions in terms of water availability to the trees. Long-term averages for the reference period 1991–2020 were calculated for each climate variable and each season. Aggregation over time was performed in Julia (Bezanson et al., 2017) using the JuliaCall interface for R (Li, 2019). In addition, the number of ice days (max. temp. < 0 °C), frost days (min. temp. < 0 °C), snow cover days (snow depth ≥ 1 cm at 07:00 h), summer days (max. temp. ≥ 25 °C) and hot days (max. temp. ≥ 30 °C) were extracted from the annually gridded 1000-m resolution DWD data.

Based on the time series of seasonal aggregates, a set of trailing moving window statistics were calculated for the lag periods of 1–5 years. According to Klap et al. (2000), stress factors can have delayed effects on defoliation up to 6 years, depending on the tree species. In this study, the moving windows were chosen to capture annual and seasonal climatic conditions, excluding higher temporal resolution and limiting the set of climatic variables to those expected to have a potential effect on mortality. This was done to limit data size and to allow interpretation of sensitive time frames in the physiological response of the trees. The final set of lagged effect variables consisted of the n-year mean of mean summer temperature, the n-year mean of maximum summer temperature, the n-year maximum of maximum summer temperature, the n-year minimum of minimum winter temperature, the n-year minimum of minimum spring temperature, the n-year mean of summer CWB sum, the n-year minimum of summer CWB sum, the n-year mean of annual CWB sum and the n-year mean of the ratio AET/PET in the growing season (spring+summer), all for n = 1, 2, 3, 4, and 5, respectively. For each of these statistics, except the AET/PET ratio, the deviation from its respective long-term average (1991–2020) was calculated by subtraction. For the day count metrics, trailing moving window sums were calculated for the same lag periods. In total, the set of climate metrics consisted of 86 potential stressors. To avoid pixel artifacts of the 1000-m resolution climate data in the 100-m resolution map products, the climate layers were disaggregated to 100-m resolution using bilinear interpolation prior to prediction.

2.2.2. Topography

Topographic metrics were computed based on a 5-m resolution digital terrain model (DTM) of the German Federal Agency for Cartography and Geodesy (source: Geobasisdaten: © GeoBasis-DE / BKG (2023)). First, the DTM was aggregated to a 100-m resolution DTM by calculating the mean of all 5-m pixels per 100-m pixel. Next, slope and aspect (in degrees) as well as topographic position index (TPI) and topographic ruggedness index (TRI) were calculated, taking into account the 8 neighbors of each 100-m pixel. Aspect was converted into the two continuous variables northness (cosinus of aspect) and eastness (sinus of aspect) ranging from -1 to 1. Topographic wetness index (TWI) was obtained from a 10-m resolution product of the Federal Research

Centre for Cultivated Plants (Julius Kühn Institut, 2017). Height above nearest drainage (HAND) was obtained from a 30-m resolution product hosted on Google Earth Engine (Donchyts et al., 2016). Both were aggregated to 100-m resolution.

2.2.3. Soil

Most of the soil metrics were derived from the 250-m resolution SoilGrids data (ISRIC, 2021; Poggio et al., 2021). The mean values of the following variables were used: bulk density of the fine earth fraction [g cm^{-3}], cation exchange capacity [cmol kg^{-1}], volumetric fraction of coarse fragments ($> 2 \text{ mm}$), nitrogen content [g kg^{-1}], soil organic carbon content [g kg^{-1}], mass fraction of clay particles ($< 0.002 \text{ mm}$), mass fraction of sand particles ($> 0.05 \text{ mm}$). Data were resampled to 100-m resolution. Values are given for six soil layers with their bottom ends at 5, 15, 30, 60, 100, and 200 cm depth. Weighted means were calculated for each variable, using layer widths as weights to aggregate values into two layers for upper (0–30 cm) and lower (30–200 cm) soil.

Values for pH were derived from the regionalization of the National Forest Soil Inventory (Scherstjanoi et al., 2021), which is available for the upper (0–30 cm) and lower (30–100 cm) soil. They were downsampled from 1000-m to 100-m resolution using bilinear interpolation. Soil thickness was derived from the average soil and sedimentary deposit layer provided by Pelletier et al. (2016). Rooting depth was derived from Fan et al. (2017). The latter two products were downsampled from 0.008333° to 100-m resolution using bilinear interpolation.

2.2.4. Land cover

Inside the forest, the proximity and cardinal direction to the nearest forest edge has an influence on microclimate, which can affect tree vitality (Buras et al., 2018; Chen et al., 1993; Matlack, 1993). Distances to roads and forest edges were derived from the OpenStreetMap (OSM) road network (OpenStreetMap contributors, 2023) and the Copernicus Dominant Leaf Type (DLT) 2018 product (Copernicus CLMS, 2020). From the OSM data, all line segments with an entry in the ‘highway’ column were selected and rasterized at 10-m resolution. Despite the name, this label does not only contain highways but any kind of road including forest roads. The Euclidean distance from each non-road pixel to the nearest road pixel was calculated. A 10-m resolution forest-non-forest raster was derived from the Copernicus DLT product. Small forest gaps were closed by applying a 5×5 pixel majority filter. Then, for each forest pixel, the Euclidean distance to the nearest non-forest pixel was calculated. Based on this distance raster, the cardinal direction (aspect) of the nearest forest edge was calculated and converted into northness (cosinus of aspect) and eastness (sinus of aspect) of the nearest forest edge. All distance and direction products were aggregated from 10-m to 100-m resolution by taking the mean. Computationally intensive steps were done with WhiteboxTools (Lindsay, 2016) using the whitebox interface for R (Wu and Brown, 2023).

2.2.5. Deposition

The deposition of air pollutants was derived from the EMEP MSC-W model of the Cooperative Programme for Monitoring and Evaluation of the Long-range Transmission of Air Pollutants in Europe (EMEP, 2023; Simpson et al., 2012). The yearly gridded data with a spatial resolution of 0.1° were used to obtain deposition of oxidized nitrogen (OXN), reduced nitrogen (RDN) and oxidized sulfur (SOX) [$\text{mg m}^{-2} \text{ yr}^{-1}$]. Dry deposition is provided as separate rasters for different vegetation types (Conif, Decid, Seminat), while wet deposition is only one raster per year. All rasters were downsampled to 100-m resolution using bilinear interpolation. The Copernicus DLT 2018 map aggregated to 100-m resolution was used as a mask for coniferous forest and broadleaved forest to assign the corresponding dry deposition values from the respective EMEP raster to each pixel. Wet deposition was then added to the dry deposition everywhere. For each location and year, trailing moving averages were calculated for periods of the previous 5 and 10 years, respectively. The available deposition data covered the years

1990–2020. The mortality model was fit for the years 1998–2022. Thus, in some cases, deposition values were not available for a few years at the beginning or end of the moving window period. In such cases, the missing values were ignored and the trailing moving averages of all available years in the periods were used.

2.3. Regression models

Logistic regression was used to model mortality rate as a function of environmental predictors. Logistic regression is a form of generalized linear model. The linear combination of multiple predictors is linked to a binary dependent variable via the logit function. The response of the model is the probability for an event to occur. Random forests and generalized additive models were tested as alternatives, but logistic regression models were found to be the only suitable approach considering all the following criteria: They are fast to fit, which is necessary for extensive feature selection and cross validation involving thousands of successive fitting iterations. They are capable of dealing with a strongly imbalanced frequency distribution of the dependent variable (many live and very few dead trees). They consist of a simple mathematical equation with a small set of coefficients and can therefore easily be transferred and implemented in other software, which is required for integrating the identified relationships in forest simulation models. And they have a smooth response function, which is also defined beyond the training data range and therefore allows for a certain degree of extrapolation beyond the known feature space. Of course, predictions beyond the known feature space should be treated with caution and should only be conducted near the margins of the training data, but for predictions under climate change conditions extrapolation capacity is a model requirement.

The binary dependent variable was the status of each tree in each year as either surviving (0) or dying (1). The majority of predictors were assumed to have monotonic relationships with mortality and were entered into the regression models as simple linear terms. However, some soil or topographic variables were considered to have potentially optimum ranges for some species, and thus U-shaped relationships with mortality. In these cases, second-order polynomial terms were used. Furthermore, a limited number of pairwise interaction terms were included in the models based on the pre-selection of important predictors.

As a result, six separate models were fit for 1) spruce (*Picea abies*), 2) pine (*Pinus sylvestris*), 3) other conifers pooled, 4) beech (*Fagus sylvatica*), 5) oak (*Quercus petraea* and *Quercus robur*) and 6) other broad-leaves pooled. For each species group, the best model was derived using stepwise forward feature selection.

2.3.1. Forward feature selection

Stepwise forward feature selection was performed using the MASS::stepAIC function in R (Venables and Ripley, 2002). The procedure starts with an intercept-only model and successively adds one predictor at a time. At each step, all potential predictors are tested and selected based on the highest improvement in the Akaike Information Criterion (AIC). The procedure stops when the AIC cannot be improved any further, or when a maximum number of allowed predictors is reached. To avoid multicollinearity between predictors, the pairwise correlation coefficients between the last added predictor and all remaining variables were calculated after each step. All variables for which this correlation coefficient was greater than 0.8 were permanently removed from the set of potential predictors.

Initial test runs showed that after a number of ten to twelve predictors was reached, the models usually did not improve anymore. In some cases, primarily site conditions and only few climate variables were selected. Such models gave high values for certain goodness-of-fit criteria because they apparently captured the spatial variability in background mortality, but without climate response they were not able to reproduce the temporal variability of mortality. To ensure that the

models captured the spatial and temporal variability of mortality, it was decided to control the order of feature selection as follows: In the first six steps, only climate variables were allowed to enter the model. In the next six steps, only site condition variables were considered. As a result, a maximum of twelve predictors per species were identified. In the final six steps of feature selection, the six most important pairwise interactions between any of the twelve predictors were allowed to enter the model. Afterwards, it was tested whether including tree age as a second-order polynomial term would improve the models. [Eickenscheidt et al. \(2019\)](#) found a significant effect of tree age on defoliation, which could also be related to mortality. All submodels, i.e. climate-only, climate+site, climate+site+interactions, and climate+site+interactions+age, were cross-validated and compared. However, since age is not available as a spatially continuous predictor variable, all further analyses and map predictions were based on the climate+site+interactions models.

2.3.2. Cross validation

To validate the predictions, several cross-validations (CV) were performed. For this purpose, the models with the best identified predictor sets were fitted repeatedly with leaving test trees out of the training. The scarcity of dead trees in the dataset made it necessary to include as many of them in the training as possible. Therefore, the leave-one-out CV approach was chosen instead of a simple k-fold CV using 100 randomly sampled test trees. The term ‘test tree’ here means the status ‘alive’ or ‘dead’ of a given tree in a given year. The test trees were sampled without replacement and with the goal to obtain approximately a 50:50 ratio of dead and alive trees. Since for several species the number of dead trees in the whole dataset barely exceeded 50, the number of test trees was limited to 100. Increasing the number of test trees beyond 100 would either mean adding the same dead trees repeatedly or adding more and more live trees, both of which would not improve the understanding of model accuracy.

Purely random sampling of 100 test trees would have resulted in a large majority of live trees and very few dead trees in the test set. Therefore, balanced sampling was performed using the inverse of the number of live and dead trees as the sampling probability, resulting in a roughly 50:50 ratio of live and dead trees in the test set. However, this does not account for the fact that the majority of tree deaths were concentrated in a few extreme years. To obtain a balanced test set of live and dead trees from extreme and normal years, another balanced sampling was performed, this time using the inverse of the number of live and dead trees per year as the sampling probability. The resulting ratios of live to dead trees using this approach may deviate somewhat further from 50:50, simply because the number of dead trees in some years was very small. To test the predictive performance of a model in new locations and new years, leave-one-location-and-time-out (LOLTO) CV is required ([Meyer et al., 2018](#)). Here, all other trees from the same field plot (across all years) and all other records from the same year (across all plots) are excluded from training, and thus the CV measures the ability of the model to generalize.

In summary, the two CV approaches can be described as follows: 1) Balanced leave-one-location-and-time-out (BLOLTO) measures the model performance for a tree at a new location and in a new year, but with the majority of test trees sampled from high mortality years, for which mortality rates are expected to be easier to predict. 2) Balanced-per-year leave-one-location-and-time-out (BYLOLTO) is the more rigorous test of model performance because it provides information about the expected prediction accuracy for trees at new locations in new years, regardless of whether we are looking at a normal or extreme year.

The single predictions and observations for the 100 test trees were combined to obtain a receiver operating characteristic (ROC) curve, by plotting the true positive rate over the false positive rate for the 100 trees when considering different mortality thresholds from 0 to 1 for declaring a tree dead. The area under the curve (AUC) was calculated using the ROCR package ([Sing et al., 2005](#)) and compared to the

calibration AUC. High AUCs close to one indicate good model performance, while low AUCs close to 0.5 indicate poor model performance.

For testing the robustness of the predicted time series, a simple k-fold CV was performed, with each fold containing all data sets from one particular year. Thus, the obtained predictions come from models which were trained with all but the target year, respectively (leave-one-year-out CV).

2.3.3. Predictor importance

The importance of each predictor in each model was quantified using the permutation feature importance approach ([Molnar, 2020](#)). In this approach, the order of values of one predictor variable is randomly permuted while all others remain in the correct order. Then, it is tested how much the accuracy of model predictions is reduced when this nonsensical predictor is used. This is quantified as the reduction in AUC. By doing this for all predictors in a model, the sensitivity of the dependent variable with respect to each predictor is tested and the predictors can be ranked in order of decreasing importance. The higher the AUC reduction, the more important a predictor is.

2.3.4. Prediction maps

Mortality maps were generated for each species group and each year from 1998 to 2022 based on the data cube. The spatial resolution of these maps is 100 m. To mask out regions where a species is absent, a remote sensing-based species map was used ([Blickensdörfer et al., 2024](#)). The original 10-m resolution species map was aggregated to produce 100-m resolution occurrence maps for each of the six species groups, which were used as masks for the mortality maps. For display purposes, the maps were further aggregated to 500-m pixels by taking the means to produce the graphics in this article. It was not possible to use the same color coding for all species groups due to the large variation in species-specific maximum mortality rates. Color scales were adjusted for each species group to best display its spatiotemporal variability in mortality. Colorblind friendly palettes from the viridis package were used ([Garnier et al., 2021](#)). Pixels where the species group is absent are displayed in black.

3. Results

Six regression models for mortality predictions were derived for the different species and species groups. The following sections present a comparison of mortality model performance for the different species, an overview of the most important explanatory variables, as well as the spatio-temporal mortality patterns in the form of maps and time series.

A total of 279,908 observations (tree-year combinations of 26,585 tree individuals) were included in the analysis, of which 82% belonged to the four major tree species in Germany ([Table A1](#)): Norway spruce (*Picea abies*, 30%), Scots pine (*Pinus sylvestris*, 28%), European beech (*Fagus sylvatica*, 17%) and sessile and pedunculate oak together (*Quercus petraea* and *robur*, 6%). Other conifer species accounted for 6% of the observations ([Table A2](#)) and other broadleaved species for 12% ([Table A3](#)). [Tables A1-A3](#) show how many individuals were observed alive and dead for each species.

3.1. Model performance

Six logistic regression models were fit for the six species groups. The models can be downloaded as R model objects along with the predicted mortality maps from 10.5281/zenodo.10805412. The accuracy of the mortality predictions was evaluated using receiver operating characteristic AUC values ([Fig. 2](#)). The best model performances were observed for beech, spruce and oak, which all showed high AUCs for the calibration data (0.94 to 0.88) as well as for the different cross-validations (0.86 to 0.77, [Fig. 2a, d, e](#)). Model performance was somewhat weaker for other conifers (0.87) and other broadleaves (0.82), especially considering the cross-validated AUCs (0.72 to 0.66, [Fig. 2c, f](#)). The

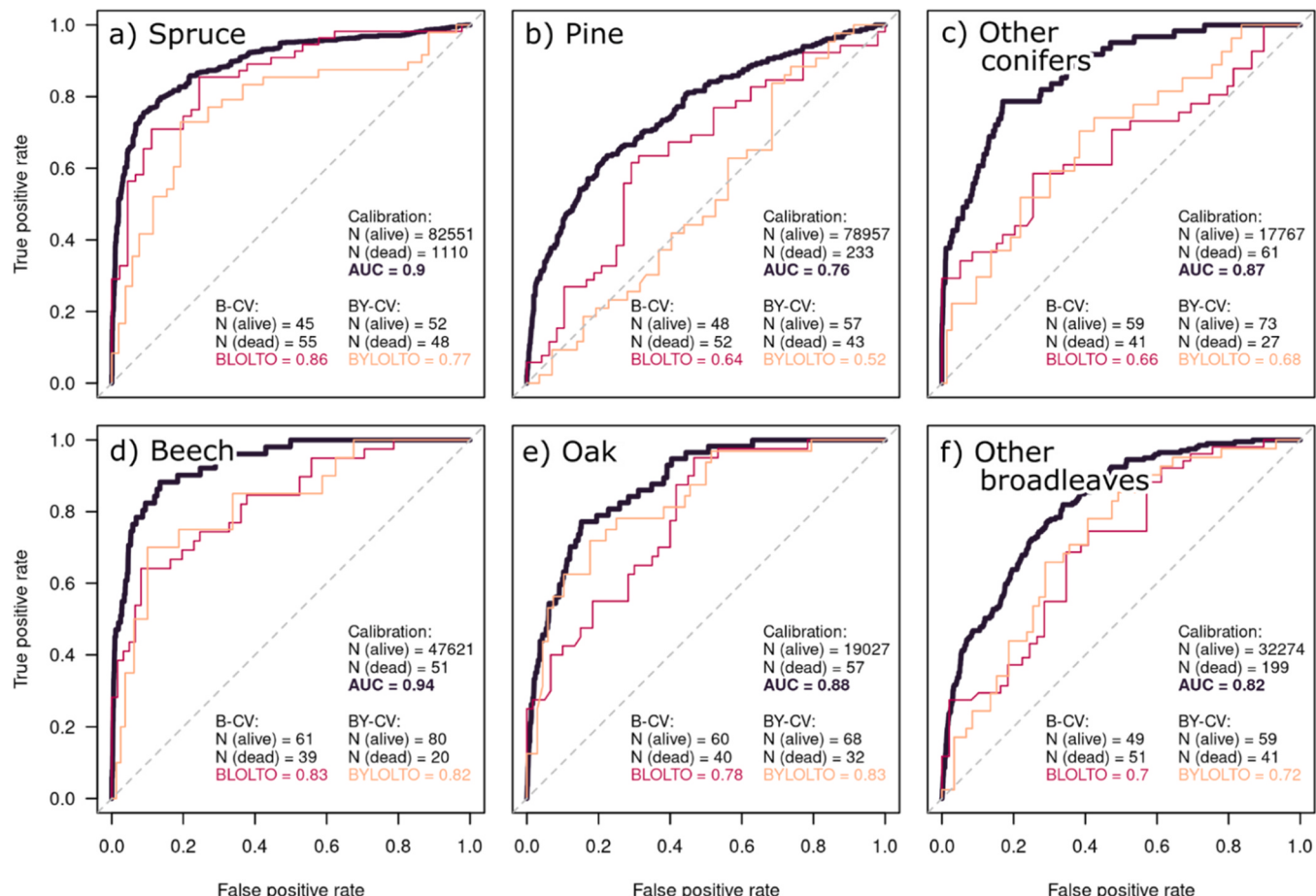


Fig. 2. Areas under the curves (AUC) for the mortality models of all six species groups. The dark bold lines represent the calibration curves, while the colored lines represent the leave-one-location-and-time-out cross-validations (LOLTO), either balanced (B-CV, red) and balanced-per-year (BY-CV, orange). N represents the number of live and dead trees, respectively.

lowest accuracy was obtained for pine, where the calibration AUC of 0.76 was still quite good, but the AUC of the strictest cross-validation (BYLOLTO) was only 0.52, barely better than random guessing (Fig. 2b).

During the model fitting process, submodels of varying complexity were obtained. While all graphs shown in this study are based on the models including climate+site+interactions, Table 1 shows how the models performed when only climate predictors were used or when climate and site predictors without interactions were used. For all species groups, model accuracies increased when site conditions and interaction terms were included in the models. This effect was strongest for beech and oak. Including tree age in the final step of the modeling resulted in slight improvements only for spruce and other broadleaves, and had no effect for the other groups.

3.2. Explanations for mortality

For each species group, a different set of predictors was identified as

most important in explaining mortality (Fig. 3). Predictor importance was measured as the reduction in AUC after random permutation of each predictor, and predictors were ranked accordingly. The strongest effects, where the AUC was reduced by 20 percentage points, were observed for beech when permuting elevation and for oak when permuting the volumetric fraction of coarse fragments in the soil. The clearest dominance, i.e. one predictor being much more important than any other, was observed for spruce, where the CWB of the driest summer in the previous 5 years had a four times stronger effect than the second most important predictor, sand content. For all species, the lowest ranking one or two predictors had little effect on the AUCs. The main findings for each species group are presented in detail in the following sections.

3.3. Spruce mortality

Since 2019, Norway spruce in Germany has shown record high mortality rates. These rates far exceeded those of any other major tree

Table 1

Areas under the curves (AUC) for mortality submodels using only subsets of predictors. AUCs are shown for calibration and in parentheses for the strictest cross-validation (BYLOLTO).

Species group	Climate-only	Climate+site	Climate+site+inter	Climate+site+inter+age
Spruce	0.85 (0.71)	0.88 (0.75)	0.9 (0.77)	0.91 (0.8)
Pine	0.7 (0.52)	0.73 (0.53)	0.76 (0.52)	-
Other conifers	0.8 (0.73)	0.84 (0.7)	0.87 (0.68)	-
Beech	0.79 (0.64)	0.86 (0.81)	0.94 (0.82)	-
Oak	0.75 (0.74)	0.82 (0.8)	0.88 (0.83)	-
Other broadleaves	0.74 (0.6)	0.8 (0.75)	0.82 (0.72)	0.84 (0.76)

Table 2

Explanations of predictor acronyms in Fig. 3.

Acronym	Explanation
rollmin	rolling minimum
rollmean	rolling mean
rollmax	rolling maximum
cwb	climatic water balance
temp	temperature
evapo	evapotranspiration
elev	elevation (altitude)
hand	height above nearest drainage
twi	topographic wetness index
tri	topographic ruggedness index
bdod	bulk density of the fine earth fraction
cfvo	volumetric fraction of coarse fragments
soc	soil organic carbon
cec	cation exchange capacity
ph_bze	pH value according to the national soil inventory (Bodenzustandserhebung)
depo	deposition
OXN	oxidized nitrogen
RDN	reduced nitrogen
SOX	oxidized sulfur

species. Before the onset of the drought in 2018, the historical mortality rate of spruce was between 0% and 2%. In 2019, the rate increased dramatically to 4%, and in 2020, 2021 and 2022 the average mortality rate of spruce across Germany was almost 10% (Fig. 4b). The most severely affected regions are located in the western and central German mountain ranges, where annual mortality rates were well above 25% (Fig. 4a).

The regression model was able to capture 99% (CV 97%) of the interannual variability in the time series and the RMSE was 0.35% (CV 0.49%; Fig. 4c). The AUC of 0.9 indicates a strong relationship between environmental factors and mortality. The almost equally high cross-validated AUCs support the strong predictive power of the model. The somewhat lower CV-AUCs when balanced per year illustrate that it is more difficult to predict spruce mortality in normal years (Fig. 2a). In drought years, however, the drought stress is the dominant effect driving the mortality response. By far, the most important predictor of spruce mortality was the CWB of the driest summer in the previous 5 years. Other important predictors were soil sand content, long-term winter temperature and mean summer temperature of the previous 5 years (Fig. 3a).

3.4. Pine mortality

Compared to Norway spruce, the mortality rate of Scots pine has increased only moderately in recent years. While the historical mortality rate for pine was typically around 0.3% until 2018, there was a spike to 1.2% in 2020, after which it fell back to levels around 0.6% (Fig. 5b). The highest rates of over 2% were observed in several regions of central and southern Germany, while in northeastern Germany, where pine is often the dominant species, mortality rates were still mostly below 1% (Fig. 5a).

The regression model was able to capture 64% (CV 30%) of the interannual variability in the time series and the RMSE was 0.15% (CV 0.24%; Fig. 5c). The AUC of 0.76 was the lowest of all species modeled. The CV-AUCs were even lower, indicating that the environmental drivers used only partially captured pine mortality. In particular, the CV-AUCs balanced per year were only slightly above 0.5, suggesting that the predictive power of the model in a random, non-drought year is very limited (Fig. 2b). The most important predictors of pine mortality were the volume of coarse fragments in the upper soil together with the mean summer CWB of the previous 4 years, the number of summer days of the previous 3 years, and the long-term spring temperature maxima (Fig. 3b).

3.5. Mortality of other conifers

The other conifers were mainly silver fir (*Abies alba*, 33%), Douglas fir (*Pseudotsuga menziesii*, 25%) and European larch (*Larix decidua*, 20%) (Table A2). In the past, the combined mortality rate for this group was usually less than 0.5%. However, it showed a first spike up to 1% in 2017, followed by a decrease to 0.6% in 2018 and 2019, and a sharp increase to 2.4% in 2020. In 2022, the rate dropped back to 0.2% (Fig. 6b). High rates > 4% were still observed at regional level in 2022, e.g. in the Black Forest and the northeastern lowlands (Fig. 6a).

The regression model was able to capture 89% (CV 51%) of the interannual variability in the time series and the RMSE was 0.17% (CV 0.34%; Fig. 6c). The AUC of 0.87 indicates a strong relationship between environmental factors and mortality. However, the CV-AUCs were somewhat lower (0.66 to 0.68), indicating the limits of the model's predictive ability. There was no clear difference between the CV with and without balancing per year, i.e. the model performed equally well in drought and non-drought years (Fig. 2c). The most important predictors of mortality of other conifers were soil organic carbon content, mean summer CWB of the previous 3 years, bulk density of the lower soil layers, and the number of summer days of the previous 4 years. Deposition of oxidized sulfur and reduced nitrogen also played a role (Fig. 3c).

3.6. Beech mortality

The background mortality of beech has been very low in past years, rarely exceeding 0.1%. There are several years in the WZE time series where no beech mortality events were observed. During the drought years, the rates increased to unusually high values, with a peak of 0.5% in 2019. In the most recent survey in 2022, the rate was 0.3% (Fig. 7b). Elevated beech mortality rates occurred mainly in the west and center of the country, while mortality rates in the south, east, and north are still close to zero in large parts (Fig. 7a).

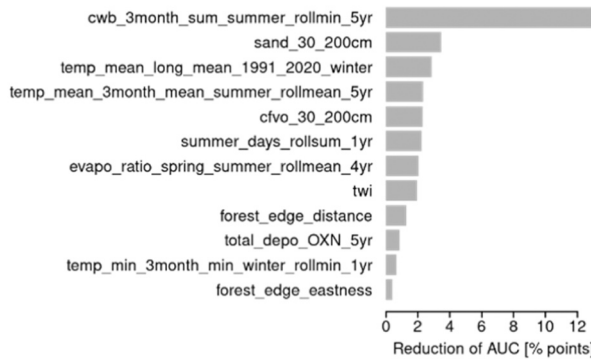
The regression model was able to capture 91% (CV 79%) of the interannual variability in the time series and the RMSE was 0.04% (CV 0.06%; Fig. 7c). The AUC of 0.94 was the highest of all species modeled. The CV-AUCs were at least 0.82 and equally good for the different balancing approaches, suggesting a very good predictive power for beech mortality in any given year (Fig. 2d). Site conditions, such as elevation, sand content, bulk density, and pH value play an important role in beech mortality. The first climate predictor, the annual CWB sum of the previous 5 years, ranks only fifth in the predictor importance ranking (Fig. 3d).

3.7. Oak mortality

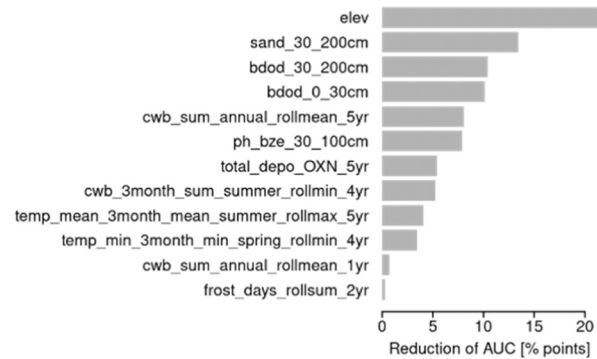
Oak mortality has fluctuated around 0.3% throughout the time series. In 2018, despite the hot and dry summer, it showed a minimum with zero dead oaks in the dataset. The highest rate was observed in 2020 with 0.7%, with a slight decrease to 0.6% in the following years (Fig. 8b). Thus, of all the species examined, oak has shown the least dramatic increase in mortality in recent years. Areas with elevated oak mortality rates above 2% can be found in a broad band from southwest to northeast Germany, while rates appear to be low in the northwestern lowlands and pre-alpine uplands (Fig. 8a).

The regression model was able to capture 73% (CV 44%) of the interannual variability in the time series and the RMSE was 0.1% (CV 0.2%; Fig. 8c). The AUC of 0.88 shows the close relationship between the predictors and oak mortality. The CV-AUCs were highest (0.83) when balanced per year, indicating good predictive power for oak mortality in any given year (Fig. 2e). Site conditions such as the volume fraction of coarse fragments in the upper soil, the height above the nearest drainage, and the clay content of the soil played the most important role in explaining oak mortality. Past deposition of reduced nitrogen was also important. The ratio of actual to potential evapotranspiration over the

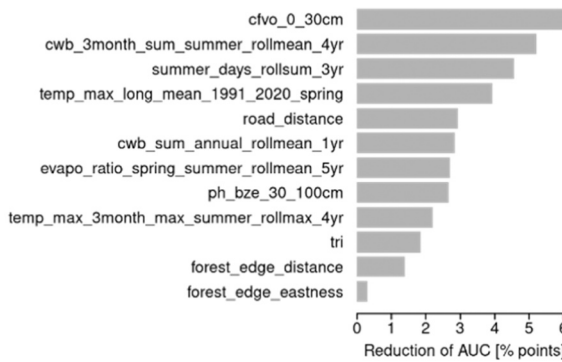
a) Spruce



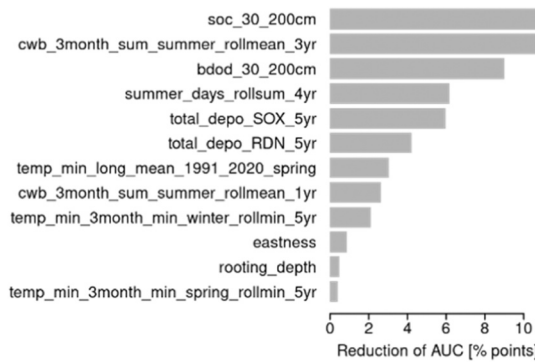
d) Beech



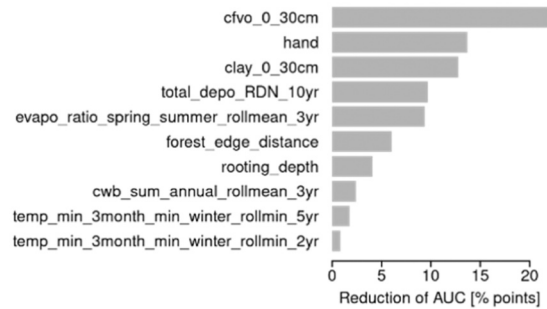
b) Pine



c) Other conifers



e) Oak



f) Other broadleaves

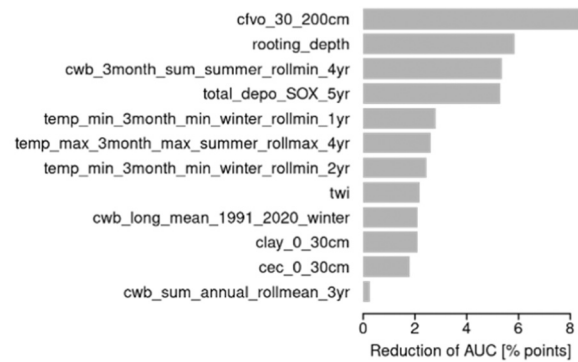


Fig. 3. Predictor importance for the six species groups obtained by predictor permutations. The larger the reduction in AUC, the more important the predictors are for accurately predicting mortality. Acronym explanations can be found in Table 2.

previous 3 growing seasons was the only climate predictor that showed a high importance for oak (Fig. 3e).

3.8. Mortality of other broadleaves

The other broadleaves were mainly black alder (*Alnus glutinosa*, 17%), European ash (*Fraxinus excelsior*, 16%), silver birch (*Betula pendula*, 15%) and sycamore maple (*Acer pseudoplatanus*, 10%; Table A3). The combined mortality rate for this group has historically been less than 0.5%. However, an increase to 1% was observed in 2014. The rate increased further to values around 2% in 2019 and 2020 and recovered somewhat to around 1.5% in 2021 and 2022 (Fig. 9b). In 2022, high rates > 4% occurred mainly in the northern German lowlands, with some hotspots in the south, notably in the Upper Rhine Valley (Fig. 9a).

The regression model was able to capture 92% (CV 85%) of the interannual variability in the time series and the RMSE was 0.16% (CV 0.24%; Fig. 9c). The AUC of 0.82 indicates a strong relationship between

environmental factors and mortality. The CV-AUCs were slightly lower (all around 0.7) with no noteworthy differences between the balancing approaches, indicating equally good model performance in drought and non-drought years (Fig. 2f). The most important predictors of mortality of other broadleaves were the volume fraction of coarse fragments in the lower soil, the rooting depth, the CWB of the driest summer of the previous 4 years and the deposition of oxidized sulfur (Fig. 3f).

4. Discussion

In the following sections, the model performance of the different species and groups will be compared and discussed in the context of known mortality mechanisms. General patterns of mortality drivers will be identified and the potential contribution of other variables, currently unavailable for modeling, will be outlined.

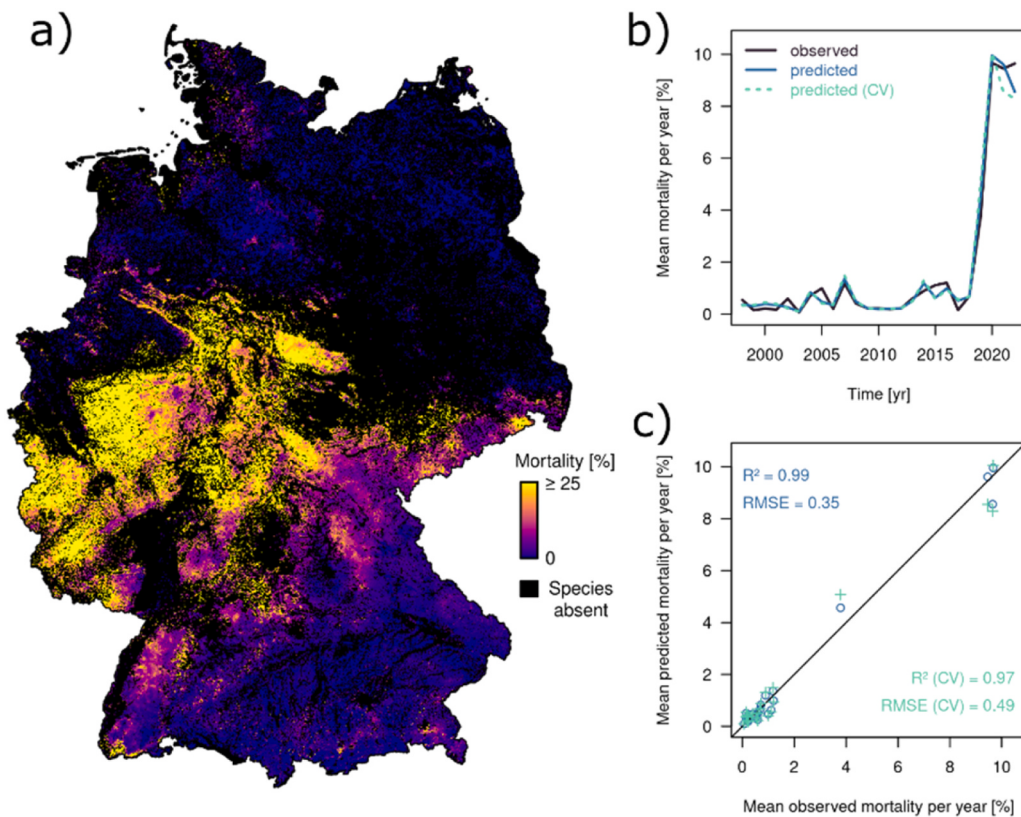


Fig. 4. Mortality of spruce (*Picea abies*) in Germany. a) Map of mortality rates in 2022 with black areas indicating absence of the species, b) time series of average mean mortality per year [%], c) 1:1-plot of predicted versus observed annual mortality. In b) and c), blue represents predictions with the full model, while green represents cross-validated predictions with the target year excluded from training.

4.1. Model assessment

According to the AUC statistics, the models for spruce, beech and oak were all very good at predicting live and dead trees in drought and non-drought years ($AUC (\text{BYLOLTO}) \geq 0.77$). The time series predictions were very good for spruce ($R^2 = 0.99$; $R^2 (\text{CV}) = 0.97$), good for beech ($R^2 = 0.91$; $R^2 (\text{CV}) = 0.79$), and somewhat weaker for oak ($R^2 = 0.73$, $R^2 (\text{CV}) = 0.44$). The response to drought among these three species decreases in this order, while the contribution of permanent site conditions in explaining mortality increases. Of all the single species models, the one for pine clearly showed the weakest performance ($AUC (\text{BLOLTO}) = 0.64$), in particular when cross-validated with an emphasis on non-drought years ($AUC (\text{BYLOLTO}) = 0.52$). Still, the overall pattern of the time series for pine was captured to a fair degree ($R^2 = 0.64$). The pine model appeared to be rather sensitive to climate legacy effects, as the spikes in the mortality time series were shifted by one year when the target year was taken out of the training during cross-validation ($R^2 (\text{CV}) = 0.3$). Model performance for the mixed species groups was weaker than for the well performing single species models. Difficulties associated with pooling ecologically different species will be discussed in Section 4.2.

There are various uncertainties associated with model predictions. The $16 \text{ km} \times 16 \text{ km}$ sampling grid of the WZE may be too coarse to capture the effects of more rarely occurring conditions, such as southern slopes. It may also miss regionally constrained effects in small geographic regions or areas with lower abundance of a particular species. For example, the pine model was able to reproduce the coarse patterns of comparatively low pine mortality in northeastern Germany and higher mortality in Bavaria, which is consistent with observations in those regions, but it was unable to predict the high pine mortality reported from the Upper Rhine Plain. It should be noted that, despite the large data set of the Crown Condition Survey, tree mortality events are

still rather rare events and the number of observed tree deaths was low for most species.

In addition to the data scarcity, there are also uncertainties associated with the predictor variables. Many of them are themselves interpolations or model products with their own prediction errors (Poggio et al., 2021). Thus, spatial predictions should be treated with caution and can be improved in the future by considering additional data sources and other factors. While logistic regression has proven to be the best suitable modeling approach according to our requirements and experience (Section 2.3), alternative modeling approaches could help to integrate more complicated relationships and predictor interactions in future studies.

4.2. Mortality mechanisms of trees

All major tree species in Germany showed increased mortality rates during the drought years 2018–2020. However, the species and groups studied differed quite strongly in the overall magnitude of mortality, the temporal and spatial patterns of mortality rates, the degree of recovery after 2020, and the environmental factors that explained most of the variability. To understand these patterns, we need to look at the ecology of the different species and groups, including their major biotic damaging agents.

The definition of mortality in managed forest ecosystems can be controversial. Should it include only standing dead trees, or should it include sanitary cutting (as in this study), thinning, or even harvesting? There is good evidence that trees removed in sanitary cuttings would have died anyway, as their attributes and past vitality values are much more similar to dead trees than to living or harvested trees (Lech and Kamińska, 2024). However, under unmanaged conditions without selective thinning, competitive self-thinning and hence natural mortality would be higher. Thus, excluding planned tree removals from mortality

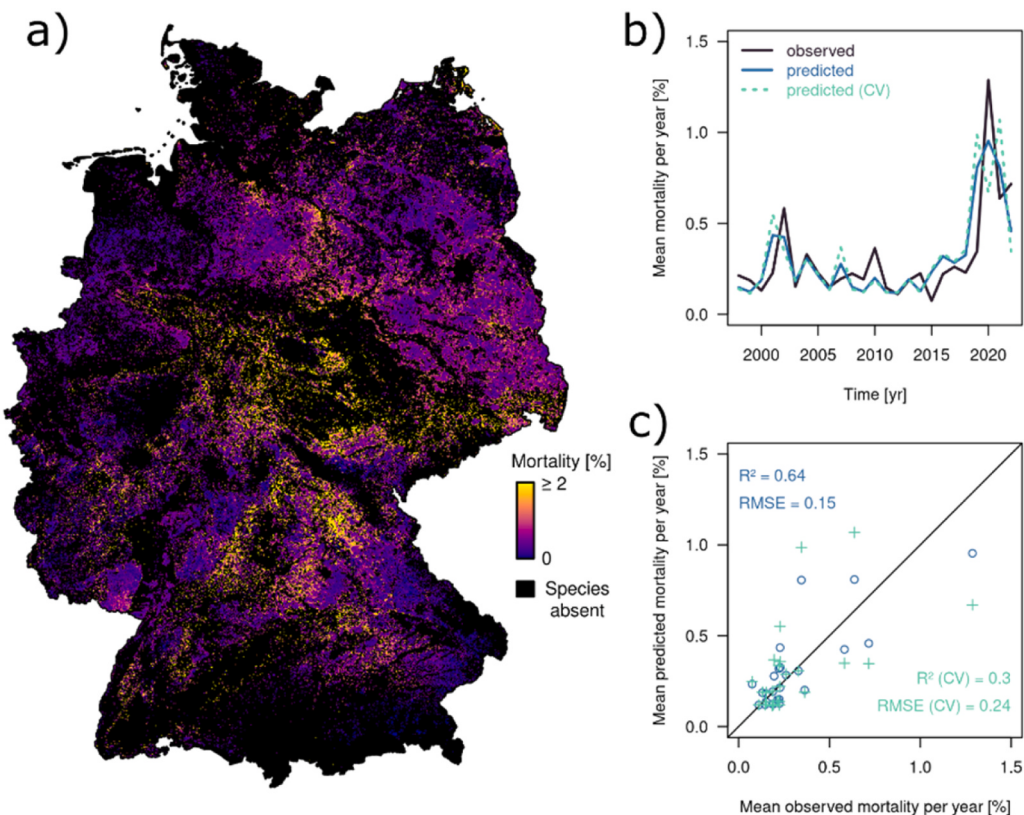


Fig. 5. Mortality of pine (*Pinus sylvestris*) in Germany. a) Map of mortality rates in 2022 with black areas indicating absence of the species, b) time series of average mortality, c) 1:1-plot of predicted versus observed annual mortality. In b) and c), blue represents predictions with the full model, while green represents cross-validated predictions with the target year excluded from training.

calculations will inevitably result in a mortality rate that must be interpreted as the lower bound of a potentially higher natural mortality. Aside from logging and disturbances such as fire and storm events, there are three main mechanisms of tree mortality: 1) hydraulic failure, 2) carbon starvation, and 3) damages by biotic agents, all of which are related to water stress during drought (Hartmann et al., 2022; McDowell et al., 2008). Two opposing strategies for coping with water stress have been described in the literature (Anderegg et al., 2012; McDowell et al., 2008; Roman et al., 2015; Sala et al., 2010; Sevanto et al., 2014): Isohydric species respond to drought by closing their stomata, limiting water loss but also gas exchange, which in turn limits photosynthesis. Over longer time periods this leads to a depletion of sugars and other carbon compounds needed to maintain defense mechanisms against insects and fungi. Anisohydric species attempt to maintain photosynthesis by keeping their stomata open at the risk of depleting all available soil water, leading to xylem embolism and eventual hydraulic failure.

4.2.1. Mortality mechanisms of major tree species

Of all the investigated tree species, spruce has undoubtedly suffered the most since 2018. On the WZE plots, 42% of the spruce trees that had been alive in 2017 were no longer alive in 2022. For all other species combined, the equivalent loss rate was 15% over the same period. The regression model clearly identified water scarcity during the summer months as the main driver of spruce mortality, confirming the sensitivity of spruce to summer drought (Solberg, 2004). Being classified as an isohydric species (Hesse et al., 2023), spruce is probably experiencing a combination of hydraulic failure and carbon starvation, resulting in high susceptibility to bark beetle infestations. The continuously high mortality rate in 2021 and 2022 is a consequence of the ongoing bark beetle dynamics. This time lag effect is reflected in the regression model by the selection of several predictors which summarize water balance or temperature over the previous four or five years. Several of the selected

predictors were summer and winter temperature metrics, which are known to be related to bark beetle development, population growth, and winter survival (Baier et al., 2007; Hlásny et al., 2021).

Pine mortality was the least well captured by the regression models. Pine mortality showed a strong peak in 2020 and, despite recovery, has remained far above pre-2020 levels in recent years. Pine is an isohydric species like spruce. However, it appears to be more drought resistant than spruce. The vitality of pines in Germany has declined severely since 2019, with crown defoliation increasing since then (BMEL, 2023b). Biotic damaging agents such as mistletoe (*Viscum album*) are contributing to this development (Matías and Jump, 2012). Since 2015, the prevalence of mistletoe among all pines in the WZE has been between 7% and 10%. In the pine regression model, several of the drought and heat predictors were selected with different time lags, as well as distances to roads and forest edges confirming previous observations of reduced pine vitality along forest edges (Buras et al., 2018). All of this points to a situation where pines in Germany are currently struggling, but not yet dying in large numbers. The drought conditions have certainly forced pines to reduce their photosynthetic activity, making them more susceptible to parasite infections.

Beech showed the lowest mortality rates of all species studied. Site conditions played a more important role in explaining beech mortality than climatic conditions. As a result, spatial patterns of elevated mortality appear more patchy than for other species. Nevertheless, the multi-year drought led to a strong increase in beech mortality due to low water availability and high temperatures. The average vitality of beech in Germany has been declining since the 1990s and defoliation has been fluctuating around high levels since the summer heat wave of 2003 (BMEL, 2023b). As an anisohydric species, beech suffers from embolisms that form under very dry conditions and persist afterwards, leading to various legacy effects (Leuschner, 2020). As a shade species, beech also increasingly suffers from sunburn after neighboring trees have died

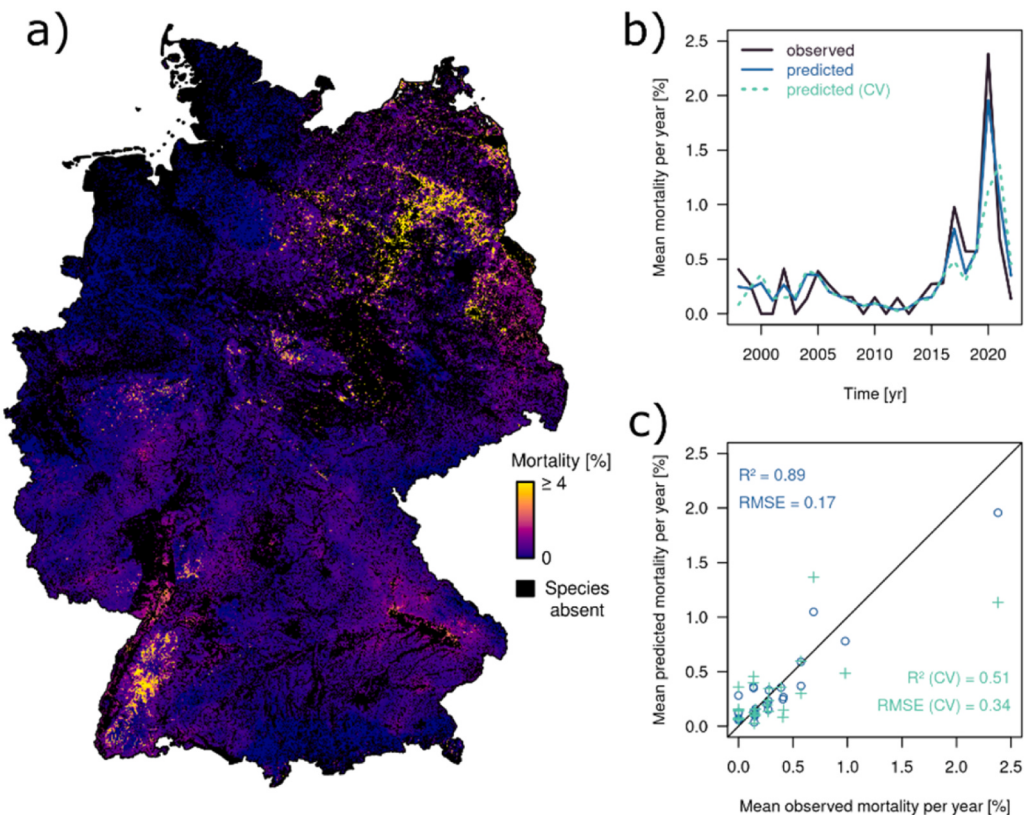


Fig. 6. Mortality of other conifer species in Germany. a) Map of mortality rates in 2022 with black areas indicating absence of the species group, b) time series of average mortality, c) 1:1-plot of predicted versus observed annual mortality. In b) and c), blue represents predictions with the full model, while green represents cross-validated predictions with the target year excluded from training.

(Brück-Dyckhoff et al., 2019). This often results in partial crown dieback and infection by fungal pathogens (Rukh et al., 2023). However, many damaged beeches also show some resilience by forming dense secondary crowns at lower heights. Therefore, the still low mortality rate of beech should not be misinterpreted as a sign of the species' vigor, but rather as a consequence of its ability to survive with severe damage. Further climate change could quickly change the situation.

Modeled oak mortality was dominated by site conditions. Climatic conditions played a minor role. Oak mortality rate was highest in 2020, but the effect of the drought was less pronounced for oak than for any other tree species studied. Peaks of similarly high rates had already occurred in 2008 and 2015. Oak vitality is known to be driven by a complex interplay of many different insect species, including leaf feeders and stem borers, other pathogens, and abiotic conditions (Haa-vik et al., 2015). Defoliation caused by insects can make trees more vulnerable to drought damage, and conversely, drought effects can make trees more susceptible to biotic attacks (Führer, 1998). High levels of defoliation have been observed in oak in Germany since the mid 1990s, with the recent drought years being no exception (BMEL, 2023b). Partial crown dieback and the formation of secondary crowns is a frequently observed phenomenon for oak in recent crown condition surveys. Thus, the mortality rate alone does not reflect the poor vitality status of the species.

4.2.2. Mortality mechanisms of other tree species

Other broadleaves and other conifers are traditionally grouped together in the annual forest condition reports because their sample sizes are considered too small for robust species-specific statistics. However, within each of the two groups very different factors may be driving the vitality and mortality of individual species. Thus, what the regression models capture is a mixture of drivers that are either important for the most abundant species in the groups or for those with

exceptionally high mortality rates. In the case of other conifers, the most abundant species were *Abies alba*, *Pseudotsuga menziesii* and *Larix decidua*. However, very high proportions of mortality events were observed for the rare non-native species *Pinus strobus* and *Pinus banksiana* (Table A2), which may have strongly influenced the model. In the case of other broadleaves, two of the four most abundant species, *Fraxinus excelsior* and *Betula pendula*, had high proportions of mortality events, while the other two, *Alnus glutinosa* and *Acer pseudoplatanus*, did not (Table A3). European ash (*F. excelsior*) is severely affected by ash dieback caused by the invasive fungus *Hymenoscyphus fraxineus* (Enderle et al., 2019). Since 2010, the average crown defoliation of ash in Germany has steadily increased from prior levels of less than 20% to nearly 40% (Thünen Institute, 2023). Ash mortality is strongly driven by this disease (Coker et al., 2019). These examples show that future modeling efforts should seek to improve our ability to predict mortality for the rare species as well. This could be achieved by collecting and analyzing additional data, e.g. through stratified densification of the monitoring grid. Trait-based modeling approaches should also be explored, as they would allow species to be pooled while accounting for their ecological differences, e.g. in terms of critical hydraulic thresholds (Choat et al., 2018).

4.3. Main drivers of tree mortality across species

Across all species, climatic and edaphic variables were the dominant factors in explaining mortality. In particular, summer climatic water balance or the ratio of actual to potential evapotranspiration together with summer temperatures or the number of summer days were important predictors. The selection of trailing averages and extremes with periods up to 5 years shows the legacy effects of drought conditions. Minimum winter and spring temperatures were also regularly observed among the important predictors. Among the soil variables,

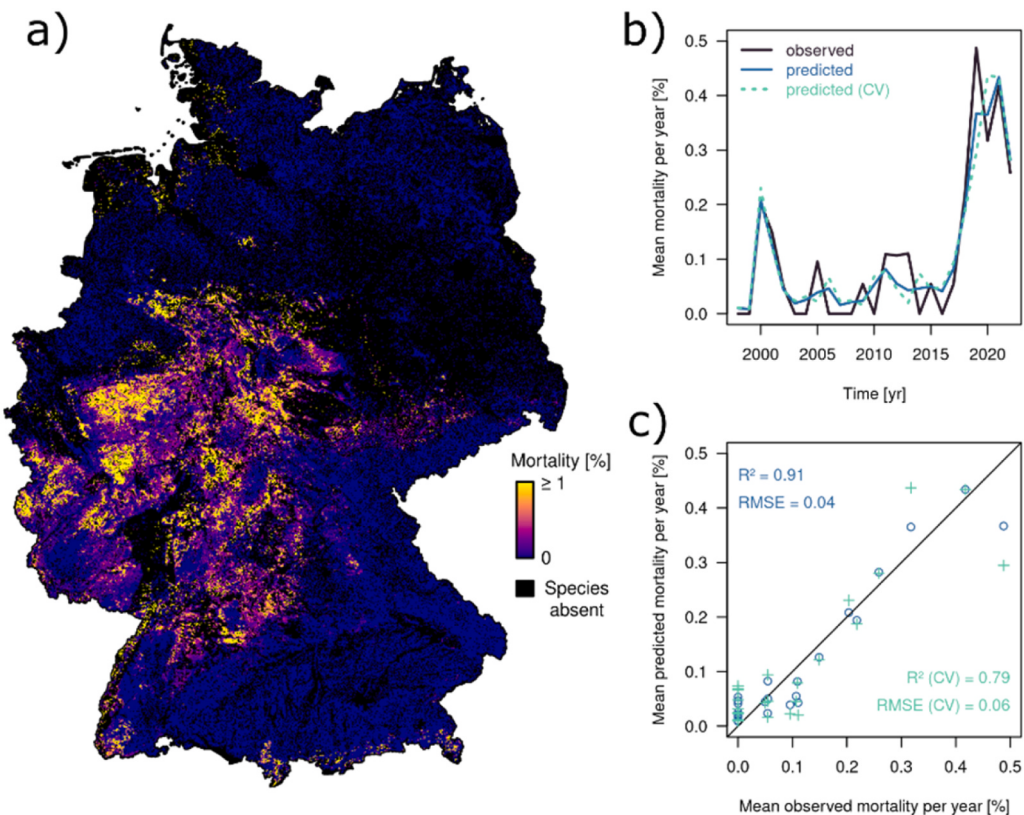


Fig. 7. Mortality of beech (*Fagus sylvatica*) in Germany. a) Map of mortality rates in 2022 with black areas indicating absence of the species, b) time series of average mortality, c) 1:1-plot of predicted versus observed annual mortality. In b) and c), blue represents predictions with the full model, while green represents cross-validated predictions with the target year excluded from training.

mainly physical parameters such as the fraction of coarse fragments, bulk density, sand and clay content, and rooting depth were selected, all of which are related to water storage capacity. Chemical soil parameters, such as pH, cation exchange capacity or carbon content appeared in only a few models. On the other hand, sulfur and nitrogen deposition, which alter soil chemistry, played a role for most species.

Surprisingly little importance was attributed to topographic predictors and distances from forest edges and roads. While elevation, height above nearest drainage, and topographic wetness index appeared to be important for some species, the cardinal direction of the topographic slope or the nearest forest edge appeared to be of little relevance. It was expected that trees on southern slopes or near south-facing forest edges, where they experience stronger sun exposition, would show higher drought mortality. Unexpectedly, the north-south orientation of slopes and forest edges did not appear in any of the models, while the respective east-west orientation did appear in some models. The fact that this study did not find an effect of northness, or more precisely southness, does not mean that it does not exist. Rather, it suggests that the Crown Condition Survey plots may not contain enough sites where such effects play a significant role.

4.4. Perspectives

A number of factors known to influence a tree's mortality risk, were not included in this study, because they were neither measured in the Crown Condition Survey nor were they available as spatial datasets with the necessary temporal resolution. One such factor is stand structure, often quantified as canopy height, vertical heterogeneity and stand density, all of which can be derived from canopy height models, e.g. from airborne laserscanning (Tymińska-Czabańska et al., 2022). The use of such information for spatial prediction over a long time series would require the existence and availability of airborne laserscanning data for

the entire study region at regular acquisition intervals. As this was not the case for Germany for the period 1998–2022, stand structure could not be included. Individual tree attributes such as stem diameter, height or age, which determine the competitive strength of a tree, can also have a significant effect on its survival (Taccoen et al., 2022). Age has been shown to strongly influence defoliation levels in the Crown Condition Survey in a previous study (Eickenscheidt et al., 2019), and individual tree age also slightly improved regression models for spruce and other broadleaves in this study. Tests also showed that age would be a stronger predictor of mortality if it were included in the forward feature selection from the start, rather than added to a model at the end after all other predictors have been fixed. However, individual tree attributes are not useful for making country-wide maps if predictions are made at the hectare scale rather than the individual tree scale. Such metrics could be interesting for modeling mortality in individual-based forest models and for building digital twins of forests.

In recent years, there has been a strong increase in satellite remote sensing activities for nationwide mapping of forest disturbances in Germany (Holzwarth et al., 2023). Maps based on time series of Sentinel-2 and Landsat data allow the quantification of canopy cover loss (Senf and Seidl, 2021b; Thonfeld et al., 2022), and temporal changes in vegetation indices have been proposed to map changes in tree vitality (Buras et al., 2021). Such top-down approaches can complement our bottom-up approach of modeling cause-effect relationships. While the bottom-up approach allows to predict mortality risk at species level based on environmental conditions, the top-down approach allows to observe where exactly the increased mortality risk is manifested in the form of dead trees.

Several remote sensing products played an important role in our study: The forest-non-forest map, from which forest edge distances and directions were calculated, the forest type map, which was used to downscale deposition, and the tree species map, which was used to mask

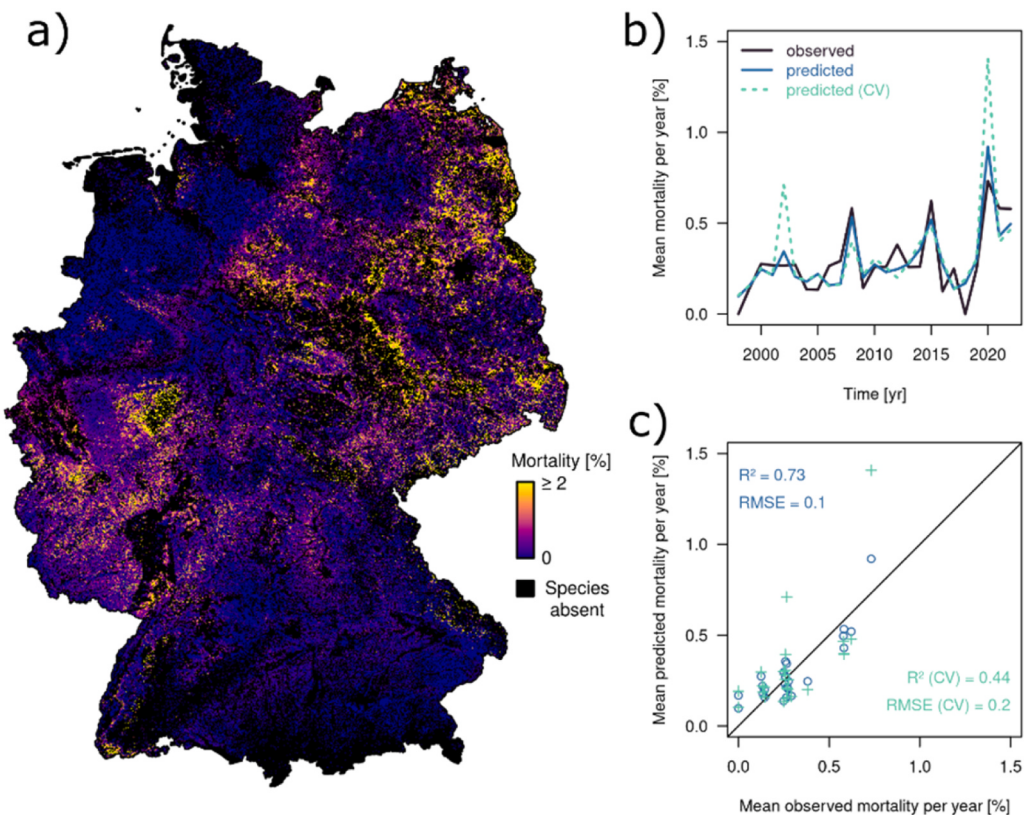


Fig. 8. Mortality of oak (*Quercus petraea* and *robur* pooled) in Germany. a) Map of mortality rates in 2022 with black areas indicating absence of the species, b) time series of average mortality, c) 1:1-plot of predicted versus observed annual mortality. In b) and c), blue represents predictions with the full model, while green represents cross-validated predictions with the target year excluded from training.

the areas where each species occurs in the mortality maps. All of these products represent the state in 2018, as this was the most recent year for which they were available. With the increased forest dynamics of recent years, such remote sensing products should be updated and published at annual resolution, as they are fundamental to any spatial modeling and forest mapping task. In particular, high-resolution species information is needed to derive regional aggregates from the mortality maps. The maps themselves provide only estimated mortality rates per hectare for a species, and need to be weighted by the area fraction of the species within each hectare to obtain correct averages.

If we want to make projections about the future development of forests under climate change, we need to consider the interplay between environment, forest growth, management and mortality. To this end, the identified relationships between environmental predictors and species-specific mortality are currently being integrated into several dynamic forest growth models (e.g., [Anders et al., in review](#)).

5. Conclusions

The study showed how mortality rates of the most important tree species in Germany can be modeled based on a number of environmental predictors. The predictive accuracy of the models was particularly high for Norway spruce, European beech and pedunculate and sessile oak. Predictions were less accurate for the mixed groups of other broadleaves and other conifers, as expected for models pooling different species, but also for Scots pine. The identified mortality drivers and their respective importance rankings were plausible and consistent with knowledge about the ecophysiology of the species. The maps provide information on the spatial patterns of mortality for each species in each year from 1998 to 2022. This is highly relevant information for quantifying the impact of the hot and dry conditions of recent years on Germany's forests on a country-wide, but especially also on a regional scale.

Furthermore, the ability to predict tree mortality for a given combination of environmental factors is crucial for planning the transition to climate-resilient forest ecosystems. The high drought-induced mortality rates of spruce indicate that large parts of the country, where spruce has been the dominant species over the past decades, are no longer suitable for the species and other, more adapted or adaptive tree species admixed or even replacing spruce should be considered by forest practitioners. The major broadleaved species beech and oak also suffered during the drought years. They require continuous monitoring to study their response and resilience to increasing frequencies of extreme conditions. The maps help with identifying suitable and unsuitable areas for these species. Further research is needed to understand the mortality drivers of pine and other species and to find suitable tree species for a sustainable management of forests in the future.

CRediT authorship contribution statement

Nikolai Knapp: Writing – review & editing, Writing – original draft, Software, Project administration, Methodology, Investigation, Formal analysis, Data curation, Conceptualization. **Nicole Wellbrock:** Writing – review & editing, Project administration, Conceptualization. **Judith Bielefeldt:** Writing – review & editing, Data curation. **Petra Dühnelt:** Writing – review & editing, Data curation. **Rainer Hentschel:** Writing – review & editing, Data curation. **Andreas Bolte:** Writing – review & editing, Conceptualization.

Declaration of Competing Interest

The authors declare the following financial interests/personal relationships which may be considered as potential competing interests: Andreas Bolte is a member of the Editorial Board of Forest Ecology and Management. All authors declare that they have no known competing

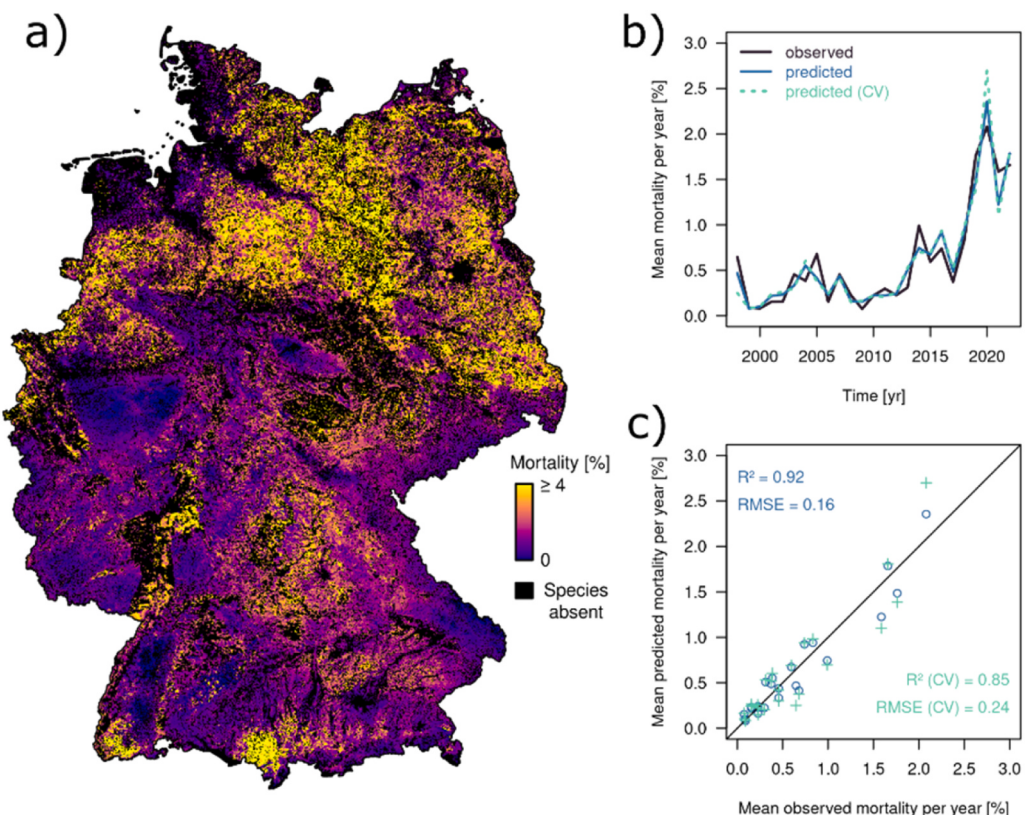


Fig. 9. Mortality of other broadleaved species in Germany. a) Map of mortality rates in 2022 with black areas indicating absence of the species group, b) time series of average mortality, c) 1:1-plot of predicted versus observed annual mortality. In b) and c), blue represents predictions with the full model, while green represents cross-validated predictions with the target year excluded from training.

financial interests or personal relationships that could have appeared to influence the work reported in this paper.

Data availability

The regression models and maps for every year from 1998 to 2022 are available under [10.5281/zenodo.10805412](https://zenodo.10805412).

Visualizations of results of the German Crown Condition Survey and underlying data are available from <https://blumwald.thuenen.de/wze/aktuelle-ergebnisse-der-wze>.

Acknowledgements

This study was funded by the German Federal Ministry of Food and

Agriculture (BMEL) through the Crown Condition Survey (WZE). We would like to thank all the people involved in the WZE who carry out field data collection, quality assurance, data management and analysis in the federal states and at national level. In particular, we thank Stefan Meining, the editor and two anonymous reviewers for helpful comments on the manuscript. We thank Fabian Schramek for testing the regression model for beech with alternative predictor data sets. We also thank the many colleagues in the scientific community with whom we discussed various ideas about the modeling approach. Finally, we thank all the contributors and the providers of the different predictor data sets for making their data available.

Appendix

Table A1 Number of observations (tree-year combinations) for the major tree species, share of the species among all observations and approximate average mortality (N dead / N total)

Species	N alive	N dead	N total	Share	Mortality
<i>Picea abies</i>	82551	1110	83661	29.889 %	1.327 %
<i>Pinus sylvestris</i>	78957	233	79190	28.291 %	0.294 %
<i>Fagus sylvatica</i>	47621	51	47672	17.031 %	0.107 %
<i>Quercus petraea</i> and <i>robur</i>	19027	57	19084	6.383 %	0.299 %

Table A2 Number of observations (tree-year combinations) for the minor conifer species, share of the species among all observations and approximate average mortality (N dead / N total)

Species	N alive	N dead	N total	Share	Mortality
<i>Abies alba</i>	5906	23	5929	2.118 %	0.388 %
<i>Pseudotsuga menziesii</i>	4403	7	4410	1.576 %	0.159 %
<i>Larix decidua</i>	3567	10	3577	1.278 %	0.280 %
<i>Larix kaempferi</i>	1807	2	1809	0.646 %	0.111 %
<i>Larix spp.</i>	647	0	647	0.231 %	0.000 %
<i>Pinus nigra</i>	379	0	379	0.135 %	0.000 %
<i>Pinus strobus</i>	318	7	325	0.116 %	2.154 %
<i>Picea sitchensis</i>	227	0	227	0.081 %	0.000 %
<i>Pinus banksiana</i>	208	11	219	0.078 %	5.023 %
<i>Abies grandis</i>	4	0	4	0.001 %	0.000 %
unspecified conifers	301	1	302	0.108 %	0.331 %

Table A3: Number of observations (tree-year combinations) for the minor broadleaved species, share of the species among all observations and approximate average mortality (N dead / N total)

Species	N alive	N dead	N total	Share	Mortality
<i>Alnus glutinosa</i>	5391	9	5400	1.929 %	0.167 %
<i>Fraxinus excelsior</i>	5117	65	5182	1.851 %	1.254 %
<i>Betula pendula</i>	4762	56	4818	1.721 %	1.162 %
<i>Acer pseudoplatanus</i>	3311	5	3316	1.185 %	0.151 %
<i>Carpinus betulus</i>	1490	1	1491	0.533 %	0.067 %
<i>Tilia cordata</i>	1321	0	1321	0.472 %	0.000 %
<i>Populus spp.</i>	851	3	854	0.305 %	0.351 %
<i>Betula pubescens</i>	914	6	920	0.329 %	0.652 %
<i>Sorbus aucuparia</i>	808	6	814	0.291 %	0.737 %
<i>Betula spp.</i>	691	6	697	0.249 %	0.861 %
<i>Prunus avium</i>	662	2	664	0.237 %	0.301 %
<i>Alnus spp.</i>	598	6	604	0.216 %	0.993 %
<i>Acer platanoides</i>	600	3	603	0.215 %	0.498 %
<i>Acer campestre</i>	600	3	603	0.215 %	0.498 %
<i>Quercus rubra</i>	578	0	578	0.206 %	0.000 %
<i>Acer spp.</i>	475	0	475	0.170 %	0.000 %
<i>Populus tremula</i>	330	4	334	0.119 %	1.198 %
<i>Salix spp.</i>	208	4	212	0.076 %	1.887 %
<i>Populus nigra</i>	153	6	159	0.057 %	3.774 %
<i>Castanea sativa</i>	150	0	150	0.054 %	0.000 %
<i>Alnus incana</i>	126	6	132	0.047 %	4.545 %
<i>Tilia spp.</i>	126	0	126	0.045 %	0.000 %
<i>Tilia platyphyllos</i>	117	0	117	0.042 %	0.000 %
<i>Robinia pseudoacacia</i>	108	0	108	0.039 %	0.000 %
<i>Sorbus aria</i>	80	0	80	0.029 %	0.000 %
<i>Ulmus spp.</i>	55	1	56	0.020 %	1.786 %
<i>Populus hybrides</i>	55	0	55	0.020 %	0.000 %
<i>Sorbus torminalis</i>	50	0	50	0.018 %	0.000 %
<i>Salix caprea</i>	37	1	38	0.014 %	2.632 %
<i>Ulmus glabra</i>	26	1	27	0.010 %	3.704 %
<i>Malus sylvestris</i>	13	0	13	0.005 %	0.000 %
<i>Ulmus effusa</i>	6	1	7	0.003 %	14.286 %
<i>Pyrus communis</i>	6	0	6	0.002 %	0.000 %
<i>Prunus serotina</i>	6	0	6	0.002 %	0.000 %
unspecified broadleaves	2453	4	2457	0.878 %	0.163 %

References

- Adams, H.D., Zeppel, M.J.B., Anderegg, W.R.L., Hartmann, H., Landhäusser, S.M., Tissue, D.T., Huxman, T.E., Hudson, P.J., Franz, T.E., Allen, C.D., Anderegg, L.D.L., Barron-Gafford, G.A., Beerling, D.J., Breshears, D.D., Brodribb, T.J., Bugmann, H., Cobb, R.C., Collins, A.D., Dickman, L.T., Duan, H., Ewers, B.E., Galiano, L., Galvez, D.A., Garcia-Forner, N., Gaylord, M.L., Germino, M.J., Gessler, A., Hacke, U. G., Hakamada, R., Hector, A., Jenkins, M.W., Kane, J.M., Kolb, T.E., Law, D.J., Lewis, J.D., Limousin, J.-M., Love, D.M., Macalady, A.K., Martinez-Vilalta, J., Mencuccini, M., Mitchell, P.J., Muss, J.D., O'Brien, M.J., O'Grady, A.P., Pangle, R.E., Pinkard, E.A., Piper, F.I., Plaut, J.A., Pockman, W.T., Quirk, J., Reinhardt, K., Ripullone, F., Ryan, M.G., Sala, A., Sevanto, S., Sperry, J.S., Vargas, R., Vennetier, M., Way, D.A., Xu, C., Yezpez, E.A., McDowell, N.G., 2017. A multi-species synthesis of physiological mechanisms in drought-induced tree mortality. *Nat. Ecol. Evol.* 1, 1285–1291. <https://doi.org/10.1038/s41559-017-0248-x>.
- Allen, R.G., Pereira, L.S., Raes, D., Smith, M., 1998. Crop evapotranspiration-Guidelines for computing crop water requirements-FAO Irrigation and drainage paper 56. FaO Rome 300, D05109.
- Anderegg, W.R.L., Berry, J.A., Smith, D.D., Sperry, J.S., Anderegg, L.D.L., Field, C.B., 2012. The roles of hydraulic and carbon stress in a widespread climate-induced forest die-off. *Proc. Natl. Acad. Sci. USA* 109, 233–237. <https://doi.org/10.1073/pnas.1107891109>.
- Anderegg, W.R.L., Hicke, J.A., Fisher, R.A., Allen, C.D., Aukema, J., Bentz, B., Hood, S., Lichstein, J.W., Macalady, A.K., McDowell, N., Pan, Y., Raffa, K., Sala, A., Shaw, J. D., Stephenson, N.L., Tague, C., Zeppel, M., 2015. Tree mortality from drought, insects, and their interactions in a changing climate. *New Phytol.* 208, 674–683. <https://doi.org/10.1111/nph.13477>.
- Anders, T., Hetzer, J., Knapp, N., Forrest, M., Tölle, M., Wellbrock, N., Hickler, T., in review. Modelling past and future drought impacts on Norway spruce forests in Germany. *Ecol. Model.*
- Baier, P., Pennerstorfer, J., Schopf, A., 2007. PHENIPS—a comprehensive phenology model of *Ips typographus* (L.) (Col., Scolytinae) as a tool for hazard rating of bark

- beetle infestation. *For. Ecol. Manag.* 249, 171–186. <https://doi.org/10.1016/j.foreco.2007.05.020>.
- Bezanson, J., Edelman, A., Karpinski, S., Shah, V.B., 2017. Julia: A Fresh Approach to Numerical Computing. *SIAM Rev.* 59, 65–98. <https://doi.org/10.1137/141000671>.
- BKG, 2023. Digitales Geländemodell Gitterweite 5 m [WWW Document]. URL (<https://dz.bkg.bund.de/index.php/default/digitales-geländemodell-gitterweite-5-m-dgm5.html>) (Accessed 9.29.23).
- BKG, 2018. Geographische Gitter für Deutschland in Lambert-Projektion [WWW Document]. URL (<https://gdz.bkg.bund.de/index.php/default/inspire/sonstige-inspire-themen/geographische-gitter-für-deutschland-in-lambert-projektion-geogitter-inspire.html>) (accessed 3.15.22).
- Blöckensdörfer, L., Oehmichen, K., Pflugmacher, D., Kleinschmit, B., Hostert, P., 2024. National tree species mapping using Sentinel-1/2 time series and German National Forest Inventory data. *Remote Sens. Environ.* 304, 114069 <https://doi.org/10.1016/j.rse.2024.114069>.
- BMEL, 2023a. Massive Schäden - Einsatz für die Wälder [WWW Document]. BMEL. URL (<https://www.bmel.de/DE/themen/wald/wald-in-deutschland/wald-trockenheit-klimawandel.html>) (Accessed 3.5.24).
- BMEL, 2023b. Ergebnisse der Waldzustandserhebung 2022, Waldzustandsbericht. Bundesministerium für Ernährung und Landwirtschaft (BMEL), Bonn.
- BMEL, 2021. Waldbericht der Bundesregierung 2021. Bundesministerium für Ernährung und Landwirtschaft, Bonn.
- Bolte, A., Ammer, C., Löf, M., Madsen, P., Nabuurs, G.-J., Schall, P., Spathelf, P., Rock, J., 2009. Adaptive forest management in central Europe: Climate change impacts, strategies and integrative concept. *Scand. J. For. Res.* 24, 473–482. <https://doi.org/10.1080/08287580903418224>.
- Bolte, A., Höhl, M., Hennig, P., Schad, T., Kroher, F., Seintsch, B., Englert, H., Rosenkranz, L., 2021. Zukunftsauflage Waldanpassung. AFZ Der WALD 12–16.
- Brodrrib, T.J., Cochard, H., Dominguez, C.R., 2019. Measuring the pulse of trees; using the vascular system to predict tree mortality in the 21st century. *Conserv. Physiol.* 7, coz046 <https://doi.org/10.1093/conphys/coz046>.
- Brück-Dyckhoff, C., Petercord, R., Schopf, R., 2019. Vitality loss of European beech (*Fagus sylvatica* L.) and infestation by the European beech splendour beetle (*Agrilus viridis* L., Buprestidae, Coleoptera). *For. Ecol. Manag.* 432, 150–156. <https://doi.org/10.1016/j.foreco.2018.09.001>.
- Bugmann, H., Seidl, R., Hartig, F., Bohn, F., Brüna, J., Cailleret, M., François, L., Heinke, J., Henrot, A.-J., Hickler, T., Hülsmann, L., Huth, A., Jacquemin, I., Kollas, C., Lasch-Born, P., Lexer, M.J., Merganic, J., Merganicová, K., Mette, T., Miranda, B.R., Nadal-Sala, D., Rammer, W., Rammig, A., Reineking, B., Roedig, E., Sabaté, S., Steinkamp, J., Suckow, F., Vaccianio, G., Wild, J., Xu, C., Reyer, C.P.O., 2019. Tree mortality submodels drive simulated long-term forest dynamics: assessing 15 models from the stand to global scale. *Ecosphere* 10, e02616. <https://doi.org/10.1002/ecs2.2616>.
- Buras, A., Rammig, A., Zang, C.S., 2021. The European forest condition monitor: using remotely sensed forest greenness to identify hot spots of forest decline. *Front. Plant Sci.* 12.
- Buras, A., Schunk, C., Zeitrag, C., Herrmann, C., Kaiser, L., Lemme, H., Straub, C., Taeger, S., Gößwein, S., Klemmt, H.-J., Menzel, A., 2018. Are Scots pine forest edges particularly prone to drought-induced mortality? *Environ. Res. Lett.* 13, 025001 <https://doi.org/10.1088/1748-9326/aaa0b4>.
- Chen, J., Franklin, J.F., Spies, T.A., 1993. Contrasting microclimates among clearcut, edge, and interior of old-growth Douglas-fir forest. *Agric. For. Meteorol.* 63, 219–237. [https://doi.org/10.1016/0168-1923\(93\)90061-L](https://doi.org/10.1016/0168-1923(93)90061-L).
- Choat, B., Brodrrib, T., Brodersen, C., Duursma, R., López, R., Medlyn, B., 2018. Triggers of tree mortality under drought and forest mortality. *Nature* 558, 531–539. <https://doi.org/10.1038/s41586-018-0240-x>.
- Coker, T.L.R., Roszypálek, J., Edwards, A., Harwood, T.P., Buffoy, L., Buggs, R.J.A., 2019. Estimating mortality rates of European ash (*Fraxinus excelsior*) under the ash dieback (*Hymenoscyphus fraxineus*) epidemic. *Plants People Planet* 1, 48–58. <https://doi.org/10.1002/ppp3.11>.
- Copernicus CLMS, 2020. Dominant Leaf Type 2018 (raster 10 m), Europe, 3-yearly, Sep. 2020 [WWW Document]. EEA Geospatial Data Cat. URL (<https://sdg.eea.europa.eu/catalogue/copernicus/api/records/7b28d3c1-b363-4579-9141-bdd09d073fd8>) (accessed 11.9.23).
- de Vries, W., Dobbertin, M.H., Solberg, S., van Dobben, H.F., Schaub, M., 2014. Impacts of acid deposition, ozone exposure and weather conditions on forest ecosystems in Europe: an overview. *Plant Soil* 380, 1–45. <https://doi.org/10.1007/s11104-014-2056-2>.
- Donchyts, G., Winsemius, H., Schellekens, J., Erickson, T., Hongkai Gao, Savenije, H., Giesen, N.V.D., 2016. Global 30m Height Above the Nearest Drainage. *EGU Gen. Assem., Geophysical Research Abstracts.* <https://doi.org/10.13140/RG.2.1.3956.8880>.
- Dowle, M., Srinivasan, A., 2023. data.table: Extension of `data.frame`.
- DWD Climate Data Center, 2023. Index of `/climate_environment/CDC/` [WWW Document]. URL (https://opendata.dwd.de/climate_environment/CDC/) (Accessed 9.29.23).
- Eichhorn, J., Roskams, P., Potočić, N., Timmermann, V., Ferretti, M., Mues, V., Szepesi, A., Durrant, D., Seletković, I., Schröck, H.-W., Nevalainen, S., Bussotti, F., Garcia, P., Wulff, S., 2020. Part IV: Visual Assessment of Crown Condition and Damaging Agents, in: Manual on Methods and Criteria for Harmonized Sampling, Assessment, Monitoring and Analysis of the Effects of Air Pollution on Forests. Thünen Institute of Forest Ecosystems, Eberswalde, p. 49.
- Eickenscheidt, N., Augustin, N.H., Weilbrock, N., 2019. Spatio-temporal modelling of forest monitoring data: Modelling german tree defoliation data collected between 1989 and 2015 for trend estimation and survey grid examination using GAMMs. *IForest* 12, 338–348. <https://doi.org/10.3832/ifor2932-012>.
- EMEP, 2023. EMEP MSC-W HOME [WWW Document]. URL (https://www.emep.int/mscw/mscw_moddata.html) (Accessed 11.9.23).
- Enderle, R., Stenlid, J., Vasaitis, R., 2019. An overview of ash (*Fraxinus spp.*) and the ash dieback disease in Europe. *CABI Rev.* 2019, 1–12. <https://doi.org/10.1079/PAVSNRR201914025>.
- Fan, Y., Miguez-Macho, G., Jobbág, E.G., Jackson, R.B., Otero-Casal, C., 2017. Hydrologic regulation of plant rooting depth. *Proc. Natl. Acad. Sci. USA* 114, 10572–10577. <https://doi.org/10.1073/pnas.1712381114>.
- Führer, E., 1998. Oak decline in Central Europe: a synopsis of hypotheses. *Proc. Popul. Dyn. Impacts Integr. Manag. For. Defoliating Insects USDA For. Serv. Gen. Tech. Rep. NE-247* 7–24.
- Garnier, Simon, Ross, Noam, Rudis, Robert, Camargo, Pedro, A., Sciaiani, Marco, Scherer, Cédric, 2021. viridis - Colorblind-Friendly Color Maps for R. <https://doi.org/10.5281/zenodo.4679424>.
- George, J.-P., Bürkner, P.-C., Sanders, T.G.M., Neumann, M., Cammalleri, C., Vogt, J.V., Lang, M., 2022. Long-term forest monitoring reveals constant mortality rise in European forests. *Plant Biol.* 24, 1108–1119. <https://doi.org/10.1111/plb.13469>.
- Haavik, L.J., Billings, S.A., Guldin, J.M., Stephen, F.M., 2015. Emergent insects, pathogens and drought shape changing patterns in oak decline in North America and Europe. *For. Ecol. Manag.* 354, 190–205. <https://doi.org/10.1016/j.foreco.2015.06.019>.
- Hammond, W.M., Yu, K., Wilson, L.A., Will, R.E., Anderegg, W.R.L., Adams, H.D., 2019. Dead or dying? Quantifying the point of no return from hydraulic failure in drought-induced tree mortality. *New Phytol.* 223, 1834–1843. <https://doi.org/10.1111/nph.15922>.
- Hartmann, H., Bastos, A., Das, A.J., Esquivel-Muelbert, A., Hammond, W.M., Martínez-Vilalta, J., McDowell, N.G., Powers, J.S., Pugh, T.A.M., Ruthrof, K.X., Allen, C.D., 2022. Climate change risks to global forest health: emergence of unexpected events of elevated tree mortality worldwide. *Annu. Rev. Plant Biol.* 73, 673–702. <https://doi.org/10.1146/annurev-plant-102820-012804>.
- Hesse, B.D., Gebhardt, T., Hafner, B.D., Hikino, K., Reitsam, A., Gigl, M., Dawid, C., Häberle, K.-H., Grams, T.E.E., 2023. Physiological recovery of tree water relations upon drought release—response of mature beech and spruce after five years of recurrent summer drought. *Tree Physiol.* 43, 522–538. <https://doi.org/10.1093/treephys/tpac135>.
- Hijmans, R.J., 2022. *Terra: Spat. Data Anal.*
- Hlášny, T., König, L., Krokane, P., Lindner, M., Montagné-Huck, C., Müller, J., Qin, H., Raffa, K.F., Schelhaas, M.-J., Svoboda, M., Viiri, H., Seidl, R., 2021. Bark Beetle outbreaks in Europe: state of knowledge and ways forward for management. *Curr. Rep.* 7, 138–165. <https://doi.org/10.1007/s40725-021-00142-x>.
- Holzwarth, S., Thonfeld, F., Kacic, P., Abdullahi, S., Asam, S., Coleman, K., Eisfelder, C., Gessner, U., Huth, J., Kraus, T., Shatto, C., Wessel, B., Kuenzer, C., 2023. Earth-observation-based monitoring of forests in Germany—recent progress and research frontiers: a review. *Remote Sens.* 15, 4234. <https://doi.org/10.3390/rs15174234>.
- ISRIC, 2021. ISRIC - Index of /soilgrids/latest/data/ [WWW Document]. URL (<https://files.isric.org/soilgrids/latest/data/>) (Accessed 10.7.21).
- Julius Kühn Institut, 2017. WMS/WFS-Dienste - Topographischer Feuchteindex - flf. julius-kuehn.de [WWW Document]. URL (<https://flf.julius-kuehn.de/webdienste/webdienste-des-flf/topographischer-feuchteindex.html>) (Accessed 9.29.23).
- Klap, J.M., Oude Voshaar, J.H., De Vries, W., Erisman, J.W., 2000. Effects of environmental stress on forest crown condition in Europe. Part IV: statistical analysis of relationships. *Water Air Soil Pollut.* 119, 387–420. <https://doi.org/10.1023/A:100515720701>.
- Knutzen, F., Averbeck, P., Barrasco, C., Bouwer, L.M., Gardiner, B., Grünzweig, J.M., Hänel, S., Haustein, K., Johannessen, M.R., Kollet, S., Pietikäinen, J.-P., Pietras-Couffignal, K., Pinto, J.G., Rechid, D., Rousi, E., Russo, A., Suarez-Gutierrez, L., Wendler, J., Xoplaki, E., Glikman, D., 2023. Impacts and damages of the European multi-year drought and heat event 2018–2020 on forests, a review. *EGUSphere* 1–56. <https://doi.org/10.5194/egusphere-2023-1463>.
- Lech, P., Kamińska, A., 2024. Mortality, or not mortality, that is the question ...: How to treat removals in tree survival analysis of central European managed forests. *Plants* 13, 248. <https://doi.org/10.3390/plants13020248>.
- Leuschner, C., 2020. Drought response of European beech (*Fagus sylvatica* L.)—a review. *Perspect. Plant Ecol. Evol. Syst.* 47, 125576. <https://doi.org/10.1016/j.ppees.2020.125576>.
- Li, C., 2019. JuliaCall: an R package for seamless integration between R and Julia. *J. Open Source Softw.* 4, 1284. <https://doi.org/10.21105/joss.01284>.
- Lindsay, J.B., 2016. Whitebox GAT: A case study in geomorphometric analysis. *Comput. Geosci.* 95, 75–84. <https://doi.org/10.1016/j.cageo.2016.07.003>.
- Matías, L., Jump, A.S., 2012. Interactions between growth, demography and biotic interactions in determining species range limits in a warming world: the case of *Pinus sylvestris*. *. Ecol. Manag.* 282, 10–22. <https://doi.org/10.1016/j.foreco.2012.06.053>.
- Matlack, G.R., 1993. Microenvironment variation within and among forest edge sites in the eastern United States. *Biol. Conserv.* 66, 185–194. [https://doi.org/10.1016/0006-3207\(93\)90004-K](https://doi.org/10.1016/0006-3207(93)90004-K).
- McDowell, N., Pockman, W.T., Allen, C.D., Breshears, D.D., Cobb, N., Kolb, T., Plaut, J., Sperry, J., West, A., Williams, D.G., Yepez, E.A., 2008. Mechanisms of plant survival and mortality during drought: why do some plants survive while others succumb to drought? *New Phytol.* 178, 719–739. <https://doi.org/10.1111/j.1469-8137.2008.02436.x>.
- McDowell, N.G., Allen, C.D., Anderson-Teixeira, K., Aukema, B.H., Bond-Lamberty, B., Chini, L., Clark, J.S., Dietze, M., Grossiord, C., Hanbury-Brown, A., Hurtt, G.C., Jackson, R.B., Johnson, D.J., Kueppers, L., Lichstein, J.W., Ogle, K., Poulter, B., Pugh, T.A.M., Seidl, R., Turner, M.G., Uriarte, M., Walker, A.P., Xu, C., 2020.

- Pervasive shifts in forest dynamics in a changing world. *Science* 368. <https://doi.org/10.1126/science.aaz9463>.
- Meyer, H., Reudenbach, C., Hengl, T., Katurji, M., Nauss, T., 2018. Improving performance of spatio-temporal machine learning models using forward feature selection and target-oriented validation. *Environ. Model. Softw.* 101, 1–9. <https://doi.org/10.1016/j.envsoft.2017.12.001>.
- Michel, A., Kirchner, T., Prescher, A.-K., Schwärzel, K., 2022. Forest Condition in Europe: The 2022 Assessment. ICP Forests Technical Report under the UNECE Convention on Long-range Transboundary Air Pollution (Air Convention).
- Molnar, C., 2020. Interpretable Machine Learning. Lulu.com.
- Neumair, M., Ankerst, D.P., Potočić, N., Timmermann, V., Ognjenović, M., Brandl, S., Falk, W., 2022. Drought effects of annual and long-term temperature and precipitation on mortality risk for 9 common European tree species. <https://doi.org/10.1101/2022.11.10.515913>.
- OpenStreetMap contributors, 2023. Planet dump retrieved from <https://planet.osm.org/>.
- Patacca, M., Lindner, M., Lucas-Borja, M.E., Cordonnier, T., Fidej, G., Gardiner, B., Hauf, Y., Jasinevičius, G., Labonne, S., Linkevičius, E., Mahnken, M., Milanovic, S., Nabuurs, G.-J., Nagel, T.A., Nikinmaa, L., Panyatov, M., Bercak, R., Seidl, R., Ostrogović Sever, M.Z., Socha, J., Thom, D., Vuletic, D., Zudin, S., Schelhaas, M.-J., 2023. Significant increase in natural disturbance impacts on European forests since 1950. *Glob. Change Biol.* 29, 1359–1376. <https://doi.org/10.1111/gcb.16531>.
- Pebesma, E., 2018. Simple features for R: standardized support for spatial vector data. *R J.* 10, 439–446.
- Pelletier, J.D., Broxton, P.D., Hazenberg, P., Zeng, X., Troch, P.A., Niu, G.-Y., Williams, Z., Brunke, M.A., Gochis, D., 2016. A gridded global data set of soil, intact regolith, and sedimentary deposit thicknesses for regional and global land surface modeling. *J. Adv. Model. Earth Syst.* 8, 41–65. <https://doi.org/10.1002/2015MS000526>.
- Pierce, D., 2019. ncdf4: Interface to Unidata netCDF (Version 4 or Earlier) Format Data Files.
- Poggio, L., de Sousa, L.M., Batjes, N.H., Heuvelink, G.B.M., Kempen, B., Ribeiro, E., Rossiter, D., 2021. SoilGrids 2.0: producing soil information for the globe with quantified spatial uncertainty. *Soil* 7, 217–240. <https://doi.org/10.5194/soil-7-217-2021>.
- R Core Team, 2021. R: A Language and Environment for Statistical Computing. R Foundation for Statistical Computing, Vienna, Austria.
- Rakovec, O., Samaniego, L., Harl, V., Markonis, Y., Moravec, V., Thober, S., Hanel, M., Kumar, R., 2022. The 2018–2020 multi-year drought sets a new benchmark in Europe. *Earth's Future* 10, e2021EF002394. <https://doi.org/10.1029/2021EF002394>.
- Roman, D.T., Novick, K.A., Brzostek, E.R., Dragoni, D., Rahman, F., Phillips, R.P., 2015. The role of isohydric and anisohydric species in determining ecosystem-scale response to severe drought. *Oecologia* 179, 641–654. <https://doi.org/10.1007/s00442-015-3380-9>.
- Rukh, S., Sanders, T.G.M., Krüger, I., Schad, T., Bolte, A., 2023. Distinct responses of European beech (*Fagus sylvatica* L.) to drought intensity and length—a review of the impacts of the 2003 and 2018–2019 Drought events in central Europe. *Forests* 14, 248. <https://doi.org/10.3390/f14020248>.
- Sala, A., Piper, F., Hoch, G., 2010. Physiological mechanisms of drought-induced tree mortality are far from being resolved. *New Phytol.* 186, 274–281. <https://doi.org/10.1111/j.1469-8137.2009.03167.x>.
- Scherstjanoi, M., Grüneberg, E., Wellbrock, N., 2021. pH-Werte deutscher Böden auf Wald- und Agrarflächen, Thünen à la carte. Thünen-Institut, Bundesforschungsinstitut für Ländliche Räume, Wald und Fischerei, Braunschweig. <https://doi.org/10.3220/CA1632825232000>.
- Schwärzel, K., Seidling, W., Hansen, K., Strich, S., Lorenz, M., 2022. Part I: objectives, strategy and implementation of icp forests, in: manual on methods and criteria for harmonized sampling, assessment, monitoring and analysis of the effects of air pollution on forests. Thünen Inst. For. Ecosyst. Eberswalde 12.
- Seidl, R., Thom, D., Kautz, M., Martin-Benito, D., Peltoniemi, M., Vacchiano, G., Wild, J., Ascoli, D., Petr, M., Honkanen, J., Lexer, M.J., Trotsiuk, V., Mairotta, P., Svoboda, M., Fabrika, M., Nagel, T.A., Reyer, C.P.O., 2017. Forest disturbances under climate change. *Nat. Clim. Change* 7, 395–402. <https://doi.org/10.1038/nclimate3303>.
- Senf, C., Pfugmacher, D., Zhiqiang, Y., Sebald, J., Knorn, J., Neumann, M., Hostert, P., Seidl, R., 2018. Canopy mortality has doubled in Europe's temperate forests over the last three decades. *Nat. Commun.* 9, 4978. <https://doi.org/10.1038/s41467-018-07539-6>.
- Senf, C., Seidl, R., 2021a. Persistent impacts of the 2018 drought on forest disturbance regimes in Europe. *Biogeosciences* 18, 5223–5230. <https://doi.org/10.5194/bg-18-5223-2021>.
- Senf, C., Seidl, R., 2021b. Mapping the forest disturbance regimes of Europe. *Nat. Sustain.* 4, 63–70. <https://doi.org/10.1038/s41893-020-00609-y>.
- Sevanto, S., McDowell, N.G., Dickman, L.T., Pangle, R., Rockman, W.T., 2014. How do trees die? A test of the hydraulic failure and carbon starvation hypotheses. *Plant Cell Environ.* 37, 153–161. <https://doi.org/10.1111/pce.12141>.
- Simpson, D., Benedictow, A., Berge, H., Bergström, R., Emberson, L.D., Fagerli, H., Flechard, C.R., Hayman, G.D., Gauss, M., Jonson, J.E., Jenkins, M.E., Nyfjord, A., Richter, C., Semeena, V.S., Tsyro, S., Tuovinen, J.-P., Valdebenito, Á., Wind, P., 2012. The EMEP MSC-W chemical transport model - technical description. *Atmos. Chem. Phys.* 12, 7825–7865. <https://doi.org/10.5194/acp-12-7825-2012>.
- Sing, T., Sander, O., Beerenwinkel, N., Lengauer, T., 2005. ROCR: visualizing classifier performance in R. *Bioinformatics* 21, 3940–3941. <https://doi.org/10.1093/bioinformatics/bti623>.
- Solberg, S., 2004. Summer drought: a driver for crown condition and mortality of Norway spruce in Norway. *For. Pathol.* 34, 93–104. <https://doi.org/10.1111/j.1439-0329.2004.00351.x>.
- Spathelf, P., Ammer, C., Annighöfer, P., Bolte, A., Seifert, T., Weimar, H., 2022. Fakten zum Thema: Wälder und Holznutzung. AFZ Wald. 39–44.
- Statistisches Bundesamt (Destatis), 2023. 41261-0003: Schadholzeinschlag: Deutschland, Jahre, Einschlagsursache, Holzartengruppen, Waldeigentumsarten [WWW Document]. URL <https://www-genesis.destatis.de>.
- Stojnić, S., Suchocka, M., Benito-Garzón, M., Torres-Ruiz, J.M., Cochard, H., Bolte, A., Cocozza, C., Cvjetković, B., de Luis, M., Martinez-Vilalta, J., Ræbeld, A., Tognetti, R., Delzon, S., 2018. Variation in xylem vulnerability to embolism in European beech from geographically marginal populations. *Tree Physiol.* 38, 173–185. <https://doi.org/10.1093/treephys/tpx128>.
- Taccoen, A., Piedallu, C., Seynave, I., Gégout-Petit, A., Gégout, J.-C., 2022. Climate change-induced background tree mortality is exacerbated towards the warm limits of the species ranges. *Ann. . Sci.* 79, 23. <https://doi.org/10.1186/s13595-022-01142-y>.
- Thonfeld, F., Gessner, U., Holzwarth, S., Kriese, J., da Ponte, E., Huth, J., Kuenzer, C., 2022. A First Assessment of Canopy Cover Loss in Germany's Forests after the 2018–2020 Drought Years. *Remote Sens.* 14. <https://doi.org/10.3390/rs14030562>.
- Thornthwaite, C.W., 1948. An approach toward a rational classification of climate. *Geogr. Rev.* 38, 55–94. <https://doi.org/10.2307/210739>.
- Thünen Institute, 2023. Blumwald: Aktuelle Ergebnisse der WZE [WWW Document]. URL <https://blumwald.thuenen.de/wze/aktuelle-ergebnisse-der-wze> (accessed 11.9.23).
- Tymińska-Czabańska, L., Hawrylo, P., Janiec, P., Socha, J., 2022. Tree height, growth rate and stand density determined by ALS drive probability of Scots pine mortality. *Ecol. Indic.* 145, 109643. <https://doi.org/10.1016/j.ecolind.2022.109643>.
- Venables, W.N., Ripley, B.D., 2002. Modern Applied Statistics with S, Fourth. ed. Springer, New York.
- Wellbrock, N., Bolte, A., Flessa, H. (Eds.), 2016. Dynamik und räumliche Muster forstlicher Standorte in Deutschland: Ergebnisse der Bodenzustandserhebung im Wald 2006 bis 2008. Johann Heinrich von Thünen-Institut, DE.
- Wellbrock, N., Eickenscheidt, N., Hilbrig, L., Dühnelt, P., Holzhausen, M., Bauer, A., Dammann, I., Strich, S., Engels, F., Wauer, A., 2018. Leitfaden und Dokumentation zur Waldzustandserhebung in Deutschland, Thünen Working Paper. Braunschweig.
- Wu, Q., Brown, A., 2023. whitebox: "WhiteboxTools" R Frontend.